Lectures on Detonation Physics: Introduction to the Theory of Detonation Shock Dynamics

D. Scott Stewart
Theoretical and Applied Mechanics
University of Illinois
Urbana, Illinois 61801

August 25, 1993

Abstract

These lectures review some basic results of detonation theory and are specialized to serve as an introduction to the theory of Detonation Shock Dynamics (DSD). The theory of DSD is a time-dependent, multi-dimensional theory for the propagation of near-Chapman- Jouguet (CJ) detonations. This theory is especially relevant to applications of detonation propagation in condensed explosives and the basic dynamics in freely propagating gaseous explosives as well. The theory that we present is based on rigorous mathematical arguments and rational approximations for an assumed model of the explosive material. The material is described by the compressible, reactive Euler equations for a given equation of state and kinetic rate law for the release of exothermic, chemical energy. This theory is the basis for the engineering "Method of Detonation Shock Dynamics", that is now being used in the design of explosive systems. Lectures on the Method of Detonation Shock Dynamics are being planned as a sequel. This first set of lectures were given in the summer of 1992 at Eglin Air Force Base.

Contents

1 Outline of the Lectures

The outline of theses lectures is as follows:

- A brief description of Detonation Shock Dynamics
- The basic equations
  - The compressible, reacting Euler equations
  - The Rankine-Hugoniot (RH) relations in shock normal coordinates
  - Intrinsic shock dynamics of the RH relations represented in Cartesian coordinates
- Review of steady, 1D, Zeldovich, Neumann, Doering (ZND) theory
- Shock attached coordinates
  - General form of the governing equations
- The detonation shock speed (D_n) - curvature (κ) relationship
  - Derivation of the "master" equation on a central streamline normal to the shock surface
  - Derivation of the $D_n - \kappa$ relationship under the assumptions of small shock curvature, ($\kappa << 1$), and slow time variations ($\partial/\partial t << 1$)

In the sequel to these lectures we plan to add the following topics:

- Remarks on conditions near interfaces and suitable boundary conditions
- Properties and solution of the $D_n - \kappa$ relations. The "Method of DSD"
  - Basic dynamics of a DSD wave
  - Comparison with numerical experiment
  - Comparison with physical experiment

- Research issues
  - Extension of the theory at interfaces and for wave - wave interactions
  - Hydrodynamic stability
  - General equation of state
- Constraint of the rate equation by matching with the $D_n - \kappa$ relation
- Imbedding of DSD waves in "fast - time" dynamics

2 Introduction: A brief description of Detonation Shock Dynamics

Detonation Shock Dynamics (or DSD) is the name given to a body of multi-dimensional theory that describes the dynamics of "near- Chapman-Jouguet" detonations and is named after Whitham's theory of "Geometrical Shock Dynamics" because of the similarity of the mathematical structure of the theories.

The basic result of DSD theory is that under suitable conditions, the detonation shock in the explosive propagates according to the simple formula

$$D_n = D_{CJ} - \alpha(\kappa), \tag{1}$$

where D_n is the normal velocity of the shock surface, D_{CJ} is the 1D, steady, Chapman-Jouguet velocity for the explosive, and $\alpha(\kappa)$ is a function of curvature κ, that is determined by the material properties of the explosive. A sketch of a typical $D_n - \kappa$ relation is shown in figure 1.

The curvature used in this formula is the local shock curvature at given point on the shock, with a corresponding attached normal. The outward normal direction is defined to be positive when it is pointing in the direction of the unreacted explosive. Therefore when the curvature is positive, $\kappa > 0$ the shock shape is convex and the detonation is expanding and its surface area is increasing. Negative curvature, $\kappa < 0$, corresponds to a converging detonation with a concave shape. Figure 2 shows these cases for typical

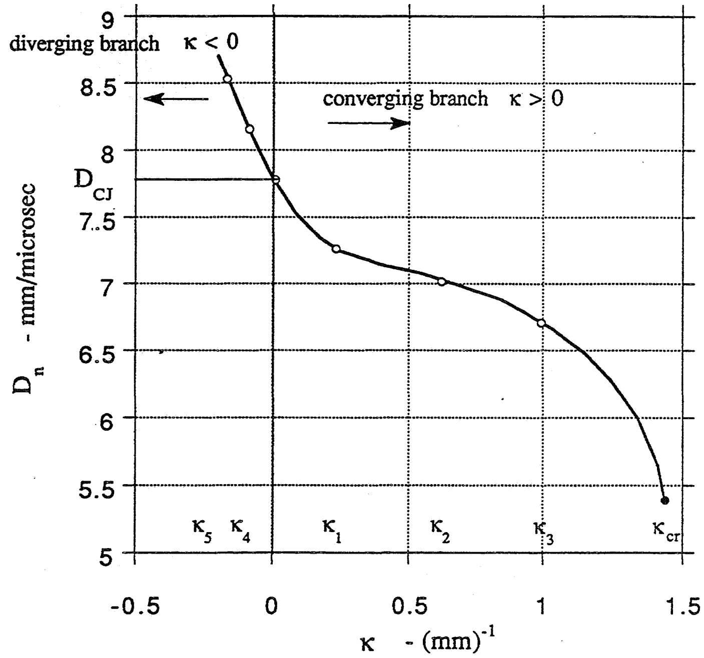

Figure 1: The $D_n - \kappa$ relation for a typical condensed phase explosive after Bdzil et. al.'s calibration of PBX 9502, [1]

detonation shocks. The detonation shock samples the curvature of the $D_n - \kappa$, relation and representative points on the detonation shock are indicated at time $t = 0$ (say) by a broken curve. The solid line shows the advancement of the shock at time $t + \triangle t$.

2.1 Surface evolution defined by the $D_n - \kappa$ relation

The $D_n - \kappa$ relation is a surface evolution equation for the detonation shock surface. Once a coordinate system is chosen, the $D_n - \kappa$ relation can be shown to be a nonlinear, parabolic partial differential equation. A simple but low resolution solution for the motion of the surface can be obtained graphically. One would discretize the surface, marking many points, at equal arclength (say) on the shock at time t, draw the local normals to the surface, measure the sum of the principle radius of curvatures , $\kappa = (\kappa_1 + \kappa_2)$ at each point on the shock surface. Then one would look up the appropriate value of D_n for the measured curvature κ_i, and then mark a new point on the normal at a distance

$$\triangle n_i = D_n(\kappa_i)\triangle t. \tag{2}$$

The advanced surface then is approximated as that one that passes through all of the new points advanced $\triangle n_i$ along their respective shock normals. This simple algorithm is equivalent to a discretized, first-order accurate numerical

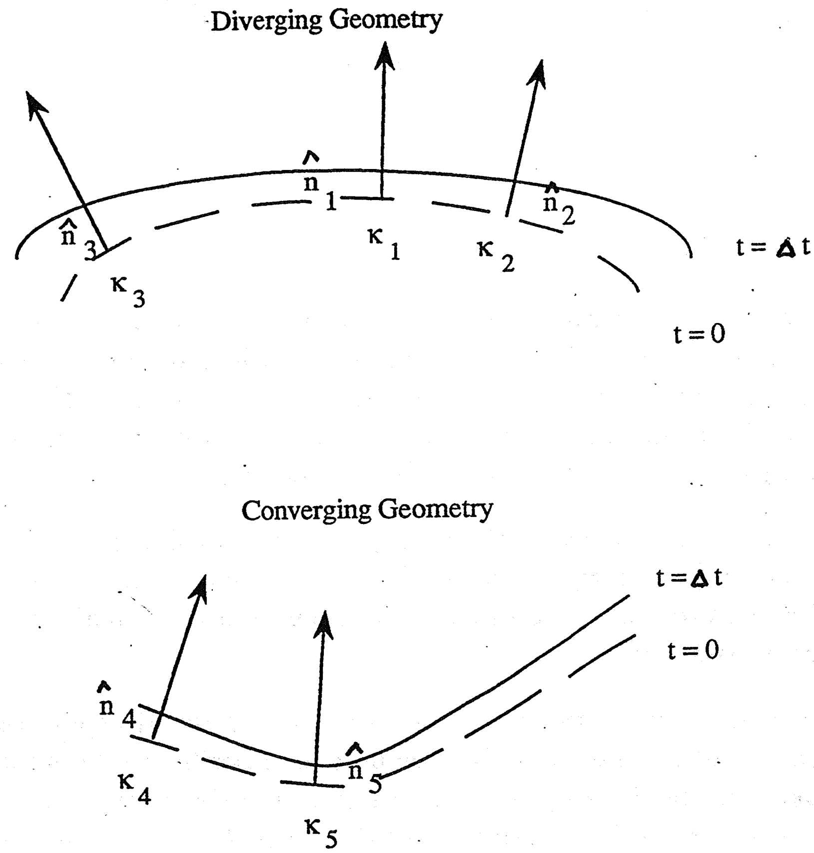

Figure 2: Figure 2a. shows a diverging portion of a near-CJ detonation shock. Figure 2b. shows a converging portion of a near-CJ detonation shock. The values of the curvature at the numbered points are indicated on the $D_n - \kappa$ curve shown in figure 1.

solution for the surface evolution equation, which is a second order partial differential equation in space and first order in time. Figure 2 indicates the graphical surface construction for a converging and diverging cases. The broken curve indicates the shock surface at the current time, t, and the solid curve indicates the shock surface at a previous time $t + \Delta t$.

Since the $D_n - \kappa$ relationship is usually monotonically decreasing with increasing curvature, regions of the detonation shock that are diverging are slowed and regions of the shock that are converging are sped up, relative to D_{CJ}.

2.2 Importance of the $D_n - \kappa$ relationship for multi-dimensional theory and application

Here we mention a few important points about the properties of the $D_n - \kappa$ relationship and their implications for basic detonation theory and explosives engineering.

- The $D_n - \kappa$ curve, combined with an analysis of the explosive confinement provided by the walls of the stick, predicts the well-known diameter effect in rate stick geometry. (The diameter effect reflects the fact that the steady axial velocity of curved detonation is a function that decreases as the stick radius decreases.)

- DSD theory shows that the $D_n - \kappa$ relationship is an intrinsic (i.e. material) property of the explosive. Therefore the $D_n - \kappa$ curve can be measured in one geometry and then be used to make predictions in other geometries.

- The $D_n - \kappa$ relationship is a correction of the Huygens construction rule that has traditionally been used to describe ideal detonation propagation. In the Huygens construction, the detonation normal velocity is constant and equal to its CJ value. The $D_n - \kappa$ relationship is found theoretically to depend on reaction zone chemistry and describes the modification of the normal detonation shock velocity from CJ. For example, the longer the 1D reaction zone is, the more important the relative reaction zone effect is on the dynamics of that explosive. This is an important consideration for insensitive high explosives that typically have long reaction zones compared to sensitive high explosives with short reaction zones.

- The shock surface evolution can be carried out with a small computational effort, when it is applicable, relative to that of direct numerical simulation. Prediction of the motion of the detonation shock surface by DSD, requires the solution of a parabolic PDE. The same simulation carried out using a Direct Numerical Simulation (DNS) of the Euler equations, requires a solution of a minimum of five (in 2D), or six (in 3D) coupled, hyperbolic equations. A more important consideration is the that the size of the simulation done for DNS is severely restricted because of accuracy limitations. DSD calculations are not limited in the same way and can be used on much larger, device-sized regions, without loss of accuracy, within the assumptions of the theory.

- The $D_n - \kappa$ relationship is sensitive to the form of the rate law (chemistry) and therefore may be an excellent experimental indicator and a way to measure the average reaction zone chemistry.

2.3 A Brief, incomplete history of the $D_n - \kappa$ relation

Here we outline some of the most important contributions to the development of the theory. This list is incomplete but indicates the main theoretical contributions.

The history of the $D_n - \kappa$ relation starts with Eyring et. al. (1949), [2] who suggested that the curvature of the detonation wave might have a significant effect on its propagation. The next important contribution was that of Wood and Kirkwood (1954), [3] who attempted to derive the relationship on a central streamtube. Their work was based on ad hoc assumptions, however they outlined the central analysis. Fickett and Davis generalized the discussion of the problem posed by Wood and Kirkwood [14] in a section of their book entitled "Slightly Divergent Flow" and used the relative velocity squared and the reaction progress variable, phase-plane. Bdzil (1981), [4] made a critical contribution that is the origin of the asymptotic theory of DSD. In his paper, Bdzil derived the diameter effect that relates the axial speed of the detonation to the diameter of the rate. To do this, he used formal asymptotic arguments based on the small reaction zone thickness compared against the diameter of the stick and established an ordinary differential equation for the steady shock shape across the stick. The steady $D_n - \kappa$ relationship is implicit in Bdzil's paper. The first asymptotic derivation of the 3D, unsteady $D_n - \kappa$ relation, was derived (and presented essentially in the form discussed in these notes) by Stewart and Bdzil (1988), [5].

Other contributions to the asymptotic theory, experimental and numerical implementation of DSD, include those of Lambourn, [6], Bukiet and Menikoff, [7], and Klein and Stewart, [8]. There have been other contributions that use ad hoc approximations that we don't mention here. Bdzil has pioneered the practical application of DSD for engineering applications, [9] and Lambourn and Swift have worked on the engineering applications in a similar effort in England [10]. A list of related references is found in the bibliography.

3 Governing Equations and the Basic Model

The basic mathematical model of explosive materials is the compressible Euler equations with reaction. A state variable theory is assumed, where the explosive is described by its thermomechanical properties for the bulk material. The basic mechanical variables are the velocity, $\vec{u}$, the density ρ and the thermodynamics pressure p. Chemistry is modeled directly in the equation of state by introducing additional thermodynamic degree(s) of freedom that measures the reaction progress of a net, forward, exothermic chemical reaction. One global progress variable, λ, can be used, but a reaction scheme can also be considered where λ is replaced by a vector λ_i. Specification of an equation of state of the form $e(p, \rho, \lambda)$ equation of state, rate law for λ (or rate laws for λ_i), is assumed to be given at the outset to describe the explosive.

3.1 Material description

3.1.1 Equation of state

In these notes, we will illustrate the DSD theory mainly for the polytropic equation of state,

$$e = \frac{p}{\rho}\frac{1}{\gamma - 1} - Q\lambda. \tag{3}$$

Here γ is the polytropic exponent and Q is the heat of combustion. This equation of state is the appropriate one for a description of a gaseous explosive. The polytropic equation of state is often used to describe the expansion of explosive products by allowing γ to have an artificially higher value than that usually allowed for gases, i.e. $\gamma \sim 2.5 - 3$. This EOS also has the advantage that a relatively large body of theoretical results exist for it. These include resolved numerical and parametric studies of the DSD theory and hydrodynamic stability, [11], [12]. DSD theory, however is not restricted to ideal EOS and nonideal explosive equations of state can be used.

For example, one might consider a typical model of an explosive that interpolates between an equation of state that matches the near-shock EOS, when $\lambda \sim 0$ and matches to the CJ products EOS when $\lambda \sim 1$ (near complete reaction). The near-shock EOS, typically of the Mie-Gruniesen form, is constructed from a Taylor series expansion in the vicinity of an experimentally determined shock Hugoniot for the unreacted explosive. This form is then guaranteed to at least fit the unreacted explosive's response to a shock. Let the near-shock EOS be $e = e_{HE}(p, \rho)$.

An example of the near-complete reaction EOS is the JWL-EOS, which is also of Mie-Gruniesen form, constructed from a Taylor series expansion that uses the CJ isentrope as a reference curve, [14]. Suppose we refer to that EOS as $e = e_{PR}(p, \rho)$. Using the reaction progress variable to provide an interpolation between the two behaviors, the composite EOS can be written in a form that resembles that for mixtures of gases, for example

$$e = (1 - \lambda)e_{HE}(p, \rho) + \lambda e_{PR}(p, \rho). \tag{4}$$

3.1.2 Burn rate law

The burn rate law, is an evolution equation for the material rate of change of the progress variable λ within the explosive material particle. The form of this rate law, derived from considerations of the microstructure, has been an uncertain element in the modeling of condensed explosives. One clear constraint is that the reaction should stop when $\lambda = 1$, which suggests that the reaction rate should be a function of, and vanishes with $1-\lambda$. The rate law is usually constrained by comparison with macroscopic physical experiment. A typical form is

$$\frac{D\lambda}{Dt} = r(p, \rho, \lambda) = k(p, \rho)(1 - \lambda)^{\nu}, \tag{5}$$

where $D\lambda/Dt$ is the material derivative of λ. Common forms for the rate premultiplier $k(p, \rho)$ include:

$$\begin{aligned}
k(p, \rho) &= \hat{k}, \text{ a constant}, & (6)\\
k(p, \rho) &= \hat{k}\ exp(-E/(p/\rho)), \text{ an Arrhenius form}, & (7)\\
k(p, \rho) &= \hat{k}\ exp(A + Bp + Cp^2), \text{ a Forest Fire form}. & (8)
\end{aligned}$$

In the above, $\hat{k}, E, A, B$ and C are constants.

In summary, the explosive's material properties are described entirely by the $e(p, \rho, \lambda)$ equation of state and the functional form for the rate law, i.e., $r(p, \rho, \lambda)$.

3.2 The conservation laws

The equations of motion are the Euler equations for a compressible, reacting material. The material or Lagrangian derivative is represented as

$$\frac{D}{Dt} \equiv \frac{\partial}{\partial t} + \vec{u} \cdot \vec{\nabla}. \tag{9}$$

The statements of conservation of mass, momentum, energy and statement and the statement that the material time rate of change of the reaction progress variable is equal to the local reaction rate are given by

$$\frac{D\rho}{Dt} + \rho \vec{\nabla} \cdot \vec{u} = 0, \tag{10}$$

$$\rho \frac{D\vec{u}}{Dt} + \vec{\nabla} p = 0, \tag{11}$$

$$\frac{De}{Dt} + p \frac{Dv}{Dt} = 0, \tag{12}$$

where $v \equiv 1/\rho$ and

$$\frac{D\lambda}{Dt} = r(p, \rho, \lambda). \tag{13}$$

These equations hold everywhere in smooth part of the flow, i.e. with smooth variations of the field variables and their first spatial derivatives. However, the flow field is generally comprised of smooth variations which are intersected by gasdynamic discontinuities such as shocks, contact discontinuities and rarefaction fans. The detonation wave, in particular has a lead shock, followed by a smoothly varying reaction zone.

3.3 Rankine-Hugoniot relations

The ZND structure of a detonation wave has a shock wave preceding a reaction zone. A sketch is shown of the pressure and progress variable is shown in figure 3. The lead shock wave is a moving boundary whose motion and location is coupled to the smooth variations behind it. If the upstream, unreacted quiescent state is known, and the motion of the shock is approximated, then in the solution scheme the shock acts as a boundary, and the values of the variables immediately behind the shock are boundary values.

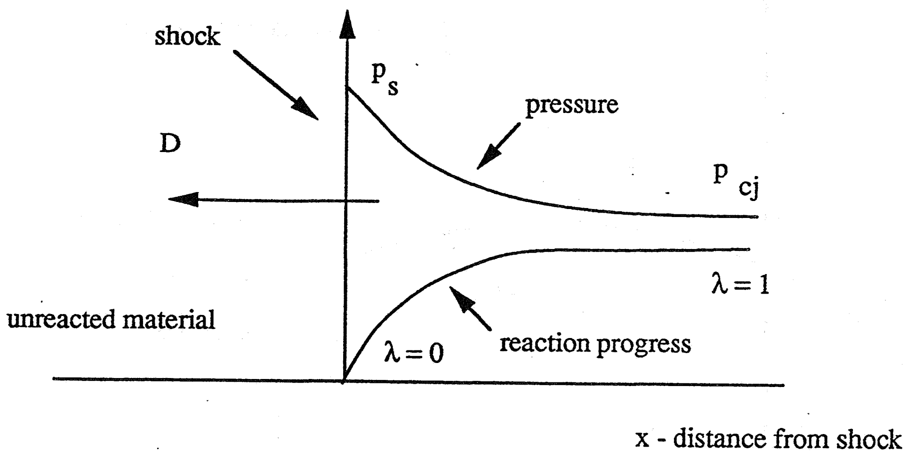

Figure 3: A sketch of the structure of a ZND detonation, which is shock wave followed by a reaction zone

3.3.1 Shock normal coordinates

The dynamics of the shock and the mathematical representation of the surface, in different coordinates systems, play a central role in the theory of DSD. The starting point of the shock surface dynamics is the Rankine-Hugoniot shock relations which conserve mass, momentum and energy of material that flows through the shock surface.

The shock is assumed to be a smooth surface of discontinuity, with an outward normal to the surface, $\hat{n}$ in the direction of the unreacted material, and with two independent vectors, $\hat{t_1}, \hat{t_2}$, in the surface of the shock, parallel to the tangent plane defined by the normal. A convenient choice defines these unit vectors, $\hat{t_i}$, in the directions of the principle radius of curvature of the surface. Figure 4 shows a 2D shock relative to laboratory coordinates. We discuss intrinsic coordinates at length in section 4.

We use a (0) subscript to denote the state in the unreacted material and use a (s) in the shocked material. Suppose that the shock surface velocity is given at each point by the vector $\vec{D}$. Let $u_n \equiv \vec{u} \cdot \hat{n}$, $u_{t_i} = \vec{u} \cdot \hat{t_i}$, $D_n \equiv \vec{D} \cdot \hat{n}$, define the normal and tangential particle velocities and the normal shock velocity. The normal mass flux m is given by $m = \rho(\vec{u} - \vec{D}) \cdot \hat{n}$. The momentum flux normal and tangential to the shock are $m(\vec{u} - \vec{D}) \cdot \hat{n}$ and $m(\vec{u}-\vec{D})\cdot\hat{t}$ respectively. Then the standard form of the normal shock relation are given by,

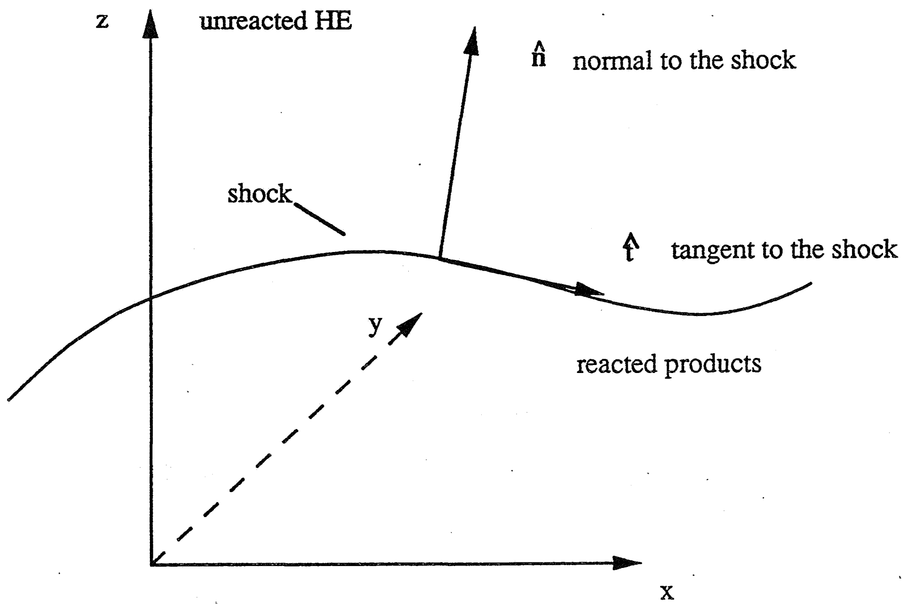

Figure 4: The geometry for a 2D detonation shock moving in a fixed laboratory coordinate system

$$[\rho(\vec{u}-\vec{D})\cdot\hat{n}]_0 = [\rho(\vec{u}-\vec{D})\cdot\hat{n}]_s \equiv m, \tag{14}$$

$$[p + m(\vec{u}-\vec{D})\cdot\hat{n}]_0 = [p + m(\vec{u}-\vec{D})\cdot\hat{n}]_s, \tag{15}$$

$$[m(\vec{D}-\vec{u})\cdot\hat{t}]_0 = [m(\vec{D}-\vec{u})\cdot\hat{t}]_s, \tag{16}$$

$$[e + p/\rho + 1/2(u_n - D_n)^2]_0 = [e + p/\rho + 1/2(u_n - D_n)^2]_s, \tag{17}$$

$$\lambda_s = 0. \tag{18}$$

Another equivalent (and convenient) form for the shock relations is

$$[\rho(u_n - D_n)]_0 = [\rho(u_n - D_n)]_s, \tag{19}$$

$$p_s - p_0 = m^2(v_0 - v_s), \tag{20}$$

$$(u_{t_i})_s = (u_{t_i})_0, \text{ for i} = 1,\ 2\ , \tag{21}$$

$$e_s - e_0 = 1/2(p_s + p_0)(v_0 - v_s), \tag{22}$$

$$\lambda_s = 0. \tag{23}$$

For a given shock equation of state, $e(p, \rho, 0)$ and for a given D_n, one can solve explicitly for the shock state, $p_s(\rho_0, p_0, D_n)$, etc. The solution for the shock state $\rho_s, (u_n)_s, (u_{t_i})_s, p_s, \lambda_s$ in terms of D_n, serves as the boundary conditions for the solution of the Euler equations. However, the velocity of the shock, D_n is ultimately determined by compatibility with the flow behind the shock and thus is part of the complete solution.

3.3.2 Exercise: Rankine Hugoniot algebra for the ideal EOS

For the ideal equation of state with reaction,

$$e = \frac{1}{\gamma - 1}\frac{p}{\rho} - Q\lambda, \tag{24}$$

define $U_n \equiv u_n - D_n$ (the relative normal velocity) and take $u_0 = 0$ so that $m = -\rho_0 D$, from the Rankine - Hugoniot relations, eliminate ρ and U in favor of p, and obtain a quadratic equation for p_s show that p_s has the solution

$$p_s = \frac{1}{\gamma+1}\left[p_0 + \frac{m^2}{\rho_0}\right] \pm \left[\left(\frac{\gamma}{\gamma+1}p_0 - \frac{1}{\gamma+1}\frac{m^2}{\rho_0}\right)^2 - \frac{\gamma-1}{\gamma+1}2m^2 Q\lambda\right]^{1/2}. \tag{25}$$

The inert shock solution is found by setting $Q\lambda = 0$. Show that when $Q\lambda = 0$ the two solutions are the undisturbed state, with $p_s/p_0 = 1$ (the minus branch) and the shock state (the plus branch) with

$$\frac{p_s}{p_0} = 1 + \frac{2\gamma}{\gamma+1}(M_0^2 - 1), \tag{26}$$

where

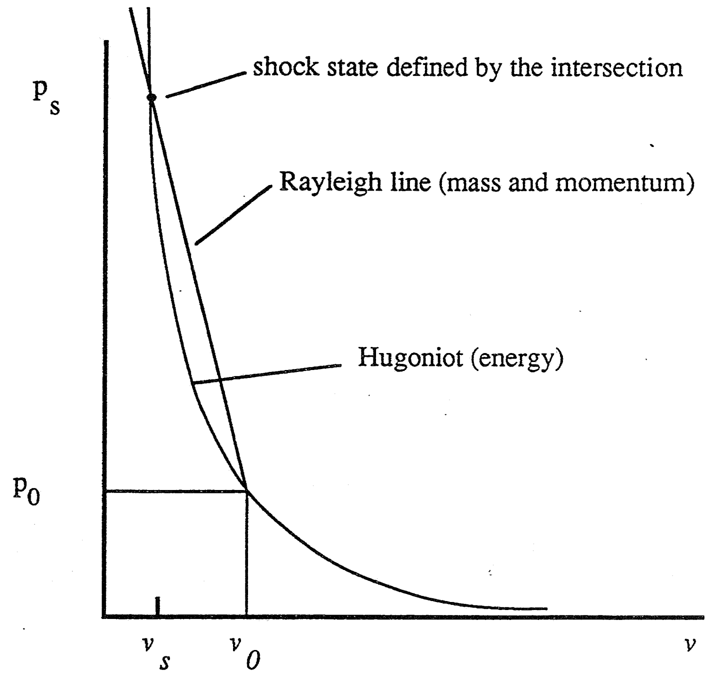

Figure 5: The Hugoniot and the Rankine line plotted in the $p-v$ plane. The intersection defines the shock state.

$$M_0^2 = \frac{D_n^2}{c_0^2}, \text{ where, } c_0^2 = \gamma p_0/\rho_0. \tag{27}$$

is the upstream Mach number of the shock.
Once the shock pressure p_s is determined, then specific volume v_s and the relative normal particle velocity, U_s are calculated by successive evaluations,

$$v_s = v_0 - \frac{p_s - p_0}{m^2}, \tag{28}$$

$$U_s = \frac{m}{\rho_s}. \tag{29}$$

The solution to the shock relations can also be obtained by graphical solution in the $p - v$ plane. One plots the Rayleigh line, (20) (a linear relationship between pressure and specific volume) and the Hugoniot curve, (22). The intersection of Rayleigh line and the Hugoniot, for $p_s/p_0 \geq 1$ defines the solution. See figure 5.

3.3.3 Exercise: Strong shock approximation

The strong shock approximation is the limit when the ratio of the shock pressure to the ambient pressure is very large, i.e.

$$\frac{p_s}{p_0} >> 1. \tag{30}$$

Show that in this limit the shock relations for the ideal equation of state reduce to,

$$\rho_s = \rho_0 \frac{\gamma+1}{\gamma-1}, \tag{31}$$

$$p_s = \frac{2}{\gamma+1}\rho_0 D_n^2, \tag{32}$$

$$U_n = u_n - D_n = -D_n \frac{\gamma-1}{\gamma+1}. \tag{33}$$

3.4 Cartesian coordinates

Consider a lab-frame Cartesian coordinate system, (similar to that shown in figure 4), where z is in the main (axial) direction of propagation of the detonation shock and the x and y axes are in the transverse directions. Suppose the shock surface is described by the surface equation

$$\psi = z - Dt - z_s(x, y, t) = 0, \tag{34}$$

where D is a constant and describes the nominally steady 1-D detonation velocity ($D = D_{CJ}$, say). Then the function $z_s(x, y, t)$ describes the deviation of the shock locus from the plane, $z = Dt$. These coordinates are useful for describing detonation in a geometry typical of a rate stick, where the detonation travels down the axis of the stick.

3.4.1 Exercise: Surface Kinematics

Given the moving surface as described above, show that the normal $\hat{n}$ is given by

$$\hat{n} = \frac{\vec{\nabla}\psi}{|\vec{\nabla}\psi|} = \frac{-\frac{\partial z_s}{\partial x}\hat{e}_x - \frac{\partial z_s}{\partial y}\hat{e}_y + \hat{e}_z}{\left[1 + \left(\frac{\partial z_s}{\partial x}\right)^2 + \left(\frac{\partial z_s}{\partial y}\right)^2\right]^{1/2}}, \tag{35}$$

and that the normal velocity of the shock surface can be written as

$$D_n\hat{n} = -\frac{1}{|\vec{\nabla}\psi|}\frac{\partial\psi}{\partial t}\hat{n}, \tag{36}$$

or

$$D_n\hat{n} = \frac{D + \frac{\partial z_s}{\partial t}}{1 + \left(\frac{\partial z_s}{\partial x}\right)^2 + \left(\frac{\partial z_s}{\partial y}\right)^2}\left(-\frac{\partial z_s}{\partial x}\hat{e}_x - \frac{\partial z_s}{\partial y}\hat{e}_y + \hat{e}_z\right). \tag{37}$$

Next, apply these specific representations to the vector form of the Rankine-Hugoniot relations, with $\vec{u} = u_x\hat{e}_x + u_y\hat{e}_y + u_z\hat{e}_z$. In particular you will need to use the mass conservation condition (which involves u_n) and the tangential momentum conservation condition (which involve the components of u_{t_i}) to obtain conditions for the jumps of u_z, u_x and u_y.

Show that in the strong shock limit, for the polytropic equation of state, in Cartesian coordinates, the Rankine-Hugoniot conditions can be solved for the shock state (s), in terms of the function $z_s(x, y, t)$ that describes the motion of the shock as

$$\rho_s = \rho_0\frac{\gamma + 1}{\gamma - 1}, \tag{38}$$

$$(u_x)_s = -\frac{2}{\gamma + 1}\left(\frac{\partial z_s}{\partial x}\right)\frac{D + \frac{\partial z_s}{\partial t}}{1 + \left(\frac{\partial z_s}{\partial x}\right)^2 + \left(\frac{\partial z_s}{\partial y}\right)^2}, \tag{39}$$

$$(u_y)_s = -\frac{2}{\gamma + 1}\left(\frac{\partial z_s}{\partial y}\right)\frac{D + \frac{\partial z_s}{\partial t}}{1 + \left(\frac{\partial z_s}{\partial x}\right)^2 + \left(\frac{\partial z_s}{\partial y}\right)^2}, \tag{40}$$

$$(u_z)_s = \frac{2}{\gamma + 1}\frac{D + \frac{\partial z_s}{\partial t}}{1 + \left(\frac{\partial z_s}{\partial x}\right)^2 + \left(\frac{\partial z_s}{\partial y}\right)^2}, \tag{41}$$

$$p_s = \frac{2}{\gamma + 1}\rho_0\left(\frac{D + \frac{\partial z_s}{\partial t}}{1 + \left(\frac{\partial z_s}{\partial x}\right)^2 + \left(\frac{\partial z_s}{\partial y}\right)^2}\right)^2, \tag{42}$$

$$\lambda_s = 0. \tag{43}$$

3.5 Dynamics of the shock interface for small shock slope

From the shock relations, we can make observations about the dynamics of the shock when the shock slope is small relative to the plane of the axial direction. To make rational approximations of the dynamics, we need to select the axial, reference normal that defines the reference tangent plane and then discuss the motion of the shock relative to it.

The smallness of the shock slope relative to the reference plane is given by the assumption that

$$\frac{\partial z_s}{\partial x} = O(\epsilon), \text{ where } \epsilon << 1. \tag{44}$$

The distortion of the shock from planar shows up in the appearance of terms, like $\partial z_s / \partial x$ in the shock jump relations. We see that shape change effects the shock state by an ordered amount. In particular, the shock pressure is changed by $O(\epsilon^2)$ from its steady 1D value by shape effect terms. The same is true for the particle velocity in the axial direction,u_z. However, the leading order correction to the transverse velocity u_x is $O(\epsilon)$.

The shock relations of the last section also show that unsteady effects of motion of the shock surface are of the same order of magnitude as the shock shape effects if the dynamics of the shock motion are sufficiently slow. The explicit assumption that shock shape and shock motion effects are comparable in their influence on the shock state is written as

$$\frac{1}{D}\frac{\partial z_s}{\partial t} \sim O(\epsilon^2). \tag{45}$$

With the assumption of the scalings given by equations (44) and (45), the expansions for the the Rankine-Hugoniot shock states for u_z, u_x and p_s take the approximate form,

$$(u_z)_s \sim \frac{2}{\gamma+1} D \left(1 + \frac{1}{D}\frac{\partial z_s}{\partial t} - \left(\frac{\partial z_s}{\partial x}\right)^2 \right), \tag{46}$$

$$(u_x)_s \sim -\frac{2}{\gamma+1} D \frac{\partial z_s}{\partial x}, \tag{47}$$

$$p_s \sim \frac{2}{\gamma+1}\rho_0 D^2 \left(1 + \frac{1}{D}\frac{\partial z_s}{\partial t} - \left(\frac{\partial z_s}{\partial x}\right)^2\right). \tag{48}$$

The expression for $(u_y)_s$ is similar to (47) and ρ_s and λ_s are unchanged from (42) and (43).

The conclusions of this section can be summarized as follows. Small spatial defects on the shock are consistent with slowly evolving dynamics. Such a theory of approximation, leads to a quasi- 1D, quasi-steady description of the detonation structure. Small shock slope corrections, $\partial z_s/\partial x \sim O(\epsilon)$ and dynamic shape changes $(\partial z_s/\partial t)/D \sim O(\epsilon^2)$ lead to

- $O(\epsilon^2)$ changes in the shock pressure
- $O(\epsilon^2)$ changes in the normal particle velocity along axial direction , (e.g u_z)
- $O(\epsilon)$ changes in the transverse particle velocities (e.g. u_x)

For this special equation of state in the strong shock limit, there are no density changes at the shock, however the density expansion follows the velocity expansion in the normal direction and the correction to the density at the shock is $O(\epsilon^2)$. The ordering scheme directly available from the shock relations suggests a specific set of scaling relations for the construction of an asymptotic theory. We use these scalings later when we derive the master equation in section 5.

4 Review of 1D, ZND Detonation Theory

The ZND theory of detonation structure assumes that the detonation is a shock wave, with a reaction zone that follows behind the shock and provides the energy that supports the detonation. From the governing equations, it is possible to find a supersonic, steady traveling wave that fits this description. The analysis of the structure of the steady ZND is the first step in a more complete, multi-dimensional theory.

To obtain the equations that describe the smoothly varying part of the detonation structure, i.e. the reaction zone, one assumes that the wave is traveling in the z-direction (say) with a fixed speed D. The particle velocities in the transverse direction are assumed to be zero and only variations in z are allowed. The wave is assumed to be steady in a traveling wave coordinate defined by $n = z - Dt$.

4.1 Exercise: Steady wave analysis

Make the following assumptions:

$$\frac{\partial}{\partial t} = \frac{\partial}{\partial x} = \frac{\partial}{\partial y} = 0, \quad \vec{u} = u_z(n)\hat{e}_z, \tag{49}$$

and let $U \equiv u_z(n) - D$. Substitute these forms into the governing equations and show that the following ODE's result

$$U\frac{d\rho}{dn} + \rho\frac{dU}{dn} = 0, \tag{50}$$

$$\rho U\frac{dU}{dn} + \frac{dp}{dn} = 0, \tag{51}$$

$$\frac{de}{dn} + p\frac{dv}{dn} = 0, \text{ with } v = 1/\rho, \tag{52}$$

$$U\frac{d\lambda}{dn} = r, \tag{53}$$

which can be written in conservative form as

$$\frac{d}{dn}(\rho U) = 0, \tag{54}$$

$$\frac{d}{dn}(p + \rho U^2) = 0, \tag{55}$$

$$\frac{d}{dn}(e + p/\rho + 1/2\,U^2) = 0, \tag{56}$$

$$\frac{d}{dn}(\lambda) = \frac{r}{U}. \tag{57}$$

(The last equation of course, is not a conservation statement, but would be if there were no reaction.)

Integration of three of the last four equations obtains

$$\rho U = C_1, \tag{58}$$

$$p + \rho U^2 = C_2, \tag{59}$$

$$e(p, \rho, \lambda) + \frac{p}{\rho} + \frac{1}{2}U^2 = C_3, \tag{60}$$

which are valid for all n within the reaction zone. In particular these equations must hold at the shock, $n = 0$. Hence by evaluating these relations at the shock, and in turn, by using the shock relations themselves, one finds (in the strong shock approximation),

$$C_1 = \rho_s U_s = -\rho_0 D, \tag{61}$$

$$C_2 = p_s + \rho_s U_s^2 = \rho_0 D^2, \tag{62}$$

$$C_3 = e(p_s, \rho_s, 0) + 1/2\, U_s^2 + p_s/\rho_s = 1/2\, D^2. \tag{63}$$

The task is to solve these relations for p, ρ and U as functions of λ and D, which in turn hold throughout the reaction zone. This is algebraically equivalent to solving the Rankine- Hugoniot shock relations, except that λ appears as a parameter and it takes on the values , $0 < \lambda < 1$ as it describes partial reaction.

Once again one can solve this problem graphically in the p, v-plane, ($v = 1/\rho$) i.e. by finding the intersection of the Rayleigh line and the partial-reacted Hugoniot. As before the Rayleigh line is given by

$$R: \; p = \frac{D^2}{v_0}\left(1 - \frac{v}{v_0}\right), \tag{64}$$

and the Hugoniot is given by

$$H: \; e(p, v, \lambda) + pv + \frac{1}{2}(v/v_0)^2 D^2 = \frac{1}{2}D^2, \tag{65}$$

which for the ideal EOS becomes

$$H : \frac{\gamma}{\gamma - 1} pv - Q\lambda + \frac{1}{2}(v/v_0)^2 D^2 = \frac{1}{2} D^2. \tag{66}$$

The negative of the slope of the Rayleigh line is proportional to the square of the detonation speed, D^2.

If one plots the Hugoniot in the p, v plane for different values of λ, the following points hold for most standard explosive equations of state.

- For partial to complete exothermic reaction, $0 \leq \lambda \leq 1$, the Hugoniot is displaced upwards, away from the origin, from the shock Hugoniot(H: evaluated with $\lambda = 0$.)

- The intersection of a Rayleigh line and the complete reaction Hugoniot, (H: evaluated with $\lambda = 1$), generally defines two solutions on the shock branch. The high pressure solution is called the Strong end state, the lower pressure solution is called the Weak end state.

- At a sufficiently small value of the detonation speed, or D^2, the Rayleigh line and the Hugoniot are tangent and the two values for the end states merge. There are no solutions for values of D below this critical value. The minimum detonation speed is called the Chapman-Jouguet detonation velocity, with $D = D_{CJ}$.

Figure 6. shows a sketch of the partial-reaction Hugoniots, Weak and Strong and CJ end states in the p, v-plane for different detonation speeds. Note that since the Rayleigh line is derived simply from the conditions of mass and momentum conservation throughout the detonation structure, it holds for each value of λ. The detonation states must lie on the Rayleigh line.

For a given value of D, such that the Rayleigh intersects the complete reaction Hugoniot, the detonation structure can be described as follows. There are two possible structures. The Weak structure has no shock and starts from the initial state, point O in figure 6, and goes up in pressure along the Rayleigh line to the Weak state. Although this structure is admissible from the point of view of being a valid solution to the governing equations, the standard argument used to rule it out is that there is no precursor ignition mechanism available to ignite the reaction zone.

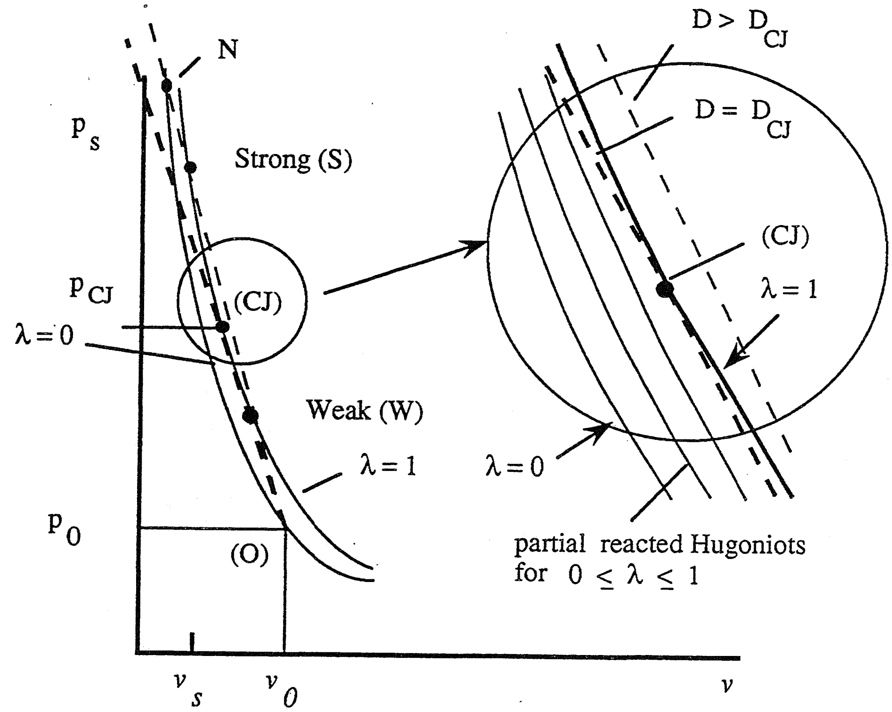

Figure 6: The p, v-plane showing partial reaction Hugoniot and the Weak, Strong and CJ state admitted by the R-H algebra. Rayleigh lines are shown as broken.

The Strong structure is called the ZND solution, and starts out with an inert shock. Thus in the p, v plane, the state jumps from point O, to the inert shock point at point N, at the intersection of the inert Hugoniot ($\lambda = 0$) and the Rayleigh line. For realistic equations of state, the shock pressure is the highest pressure within the detonation structure. The shock also provides the mechanism for the ignition of the reaction. The pressure then drops, from its highest value at state N, to its termination value at the Strong state at point S as λ increases from 0 to 1.

For a simple equation of state, these calculations can be done analytically, however for a more complex EOS the solution to the algebra must be carried out numerically. Recall that the solution for the end state pressure was in fact given in an earlier section, for the ideal EOS by equation (25). Notice that the Strong and Weak state coalesce to the CJ state when the argument of the square root vanishes.

4.2 Exercise: Calculation of D_{CJ} for the ideal EOS

Show that the condition that determines the CJ detonation velocity is easily obtained in the strong shock limit as

$$D_{CJ}^2 = 2(\gamma^2 - 1)Q. \tag{67}$$

4.3 ZND Spatial Structure

To find the spatial structure of the detonation, one still has to integrate the rate equation. We use a * subscript to denote the solution of the partial reaction Rankine-Hugoniot algebra for functions of λ

$$p = p_*(\lambda),\ U = U_*(\lambda),\ \rho = \rho_*(\lambda). \tag{68}$$

Then the rate equation is written as

$$\frac{d\lambda}{dn} = \frac{r(p_*(\lambda), \rho_*(\lambda), \lambda)}{U_*(\lambda)}, \tag{69}$$

which in turn can be integrated to obtain the spatial distribution $n = n(\lambda)$ as

$$n = \int_0^\lambda \frac{U_*(\bar{\lambda})}{r(p_*(\bar{\lambda}), \rho_*(\bar{\lambda}), \bar{\lambda})} d\bar{\lambda}. \tag{70}$$

4.3.1 Exercise: Calculation of the ZND reaction zone structure for an ideal EOS

Show that for the ideal equation of state that the CJ, ZND solution structure can be described by the relations

$$\rho_* = \rho_0 \frac{\gamma + 1}{\gamma - \ell}, \tag{71}$$

$$U_* = -D_{CJ} \frac{\gamma - \ell}{\gamma + 1}, \tag{72}$$

$$p_* = \rho_0 D_{CJ}^2 \frac{1 + \ell}{\gamma + 1}, \tag{73}$$

where ℓ is defined by

$$\ell = \sqrt{1 - \lambda}, \tag{74}$$

and that the distribution of the reactant is found from the integral of the rate equation

$$n = \int_{\ell}^{1} \frac{U_*(\hat{\ell})}{r(p_*(\hat{\ell}), \rho_*(\hat{\ell}), 1 - \hat{\ell}^2)} 2\hat{\ell} d\hat{\ell}. \tag{75}$$

Carry out the integration for the case when the rate law is given by simple depletion alone and the premultiplier of the rate constant has no state dependence. Then r is of the form

$$r = k(1 - \lambda)^{\nu}, \text{ with, } k, \nu = \text{constant}. \tag{76}$$

5 Intrinsic Geometry and Shock-Attached Coordinates

We next discuss the use of intrinsic, shock-attached coordinates, in order to describe curved, time-evolving detonation waves. Ultimately we must represent the wave system in a fixed laboratory frame which we take as (x, y, z). The intrinsic coordinate frame we discuss here has the following properties:

- The curvilinear coordinates are normal to the shock and parallel to the shock surface.
- One of the coordinate surfaces is coincident with the shock surface.
- The reaction zone follows immediately behind the shock and is accounted for in these calculations.
- The coordinates reflect the growth (or shrinkage) of the shock area (or the arc-length) in an expanding (converging) geometry.
- The coordinates are more complicated in their complete form, than Cartesian coordinates (say). This can be a disadvantage.

There are two types of intrinsic coordinates that have been developed extensively for the description of Detonation Shock Dynamics; a 2D version

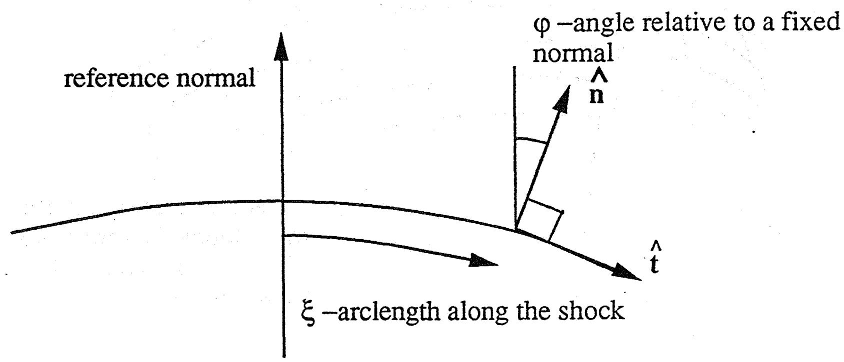

Figure 7: A sketch of arc-length angle coordinates used in 2D for DSD

that uses arc length along the shock and the angle of the shock normal relative to a fixed direction, and a 3D version that uses the orthogonal coordinate net defined by surfaces parallel to the shock surface and the lines of principle curvature defined in the shock surface itself. The first coordinates are described completely in a recent report by Bdzil and Fickett [9]. The second will be described in these notes. The presentation will be specialized, in places to 2D, to shorten the presentation. The additions required for 3D are straightforward. A representative sketch of the coordinate systems is shown in figures 7 and 8 representative of the 2D and 3D coordinate systems used in the theory.

5.1 Bertrand coordinates

The coordinates that we pick are known as Bertrand coordinates. The starting point is a shock surface that can be represented quite generally in terms of laboratory-fixed coordinates (x, y, z) as

$$\psi(x, y, z; t) = 0. \tag{77}$$

This equation constrains the lab-coordinate position vectors in the surface

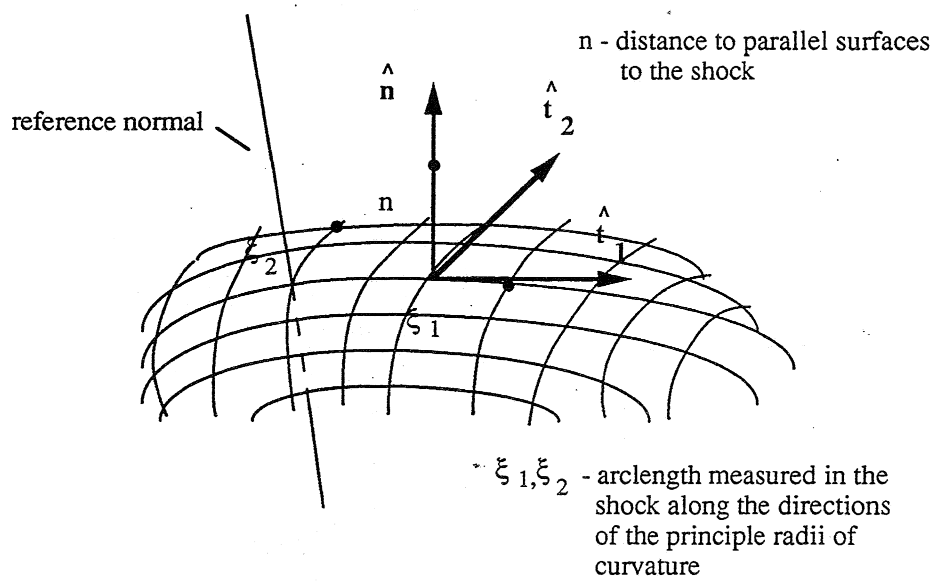

Figure 8: A sketch of the orthogonal net comprised of surfaces parallel to the shock and the surfaces aligned with the directions of principle normal curvatures in the shock surface, used for 3D, DSD theory

to

$$\vec{x} = \vec{x}_s. \tag{78}$$

The normal to the surface can always be calculated by the formula (the sign is chosen to be in the direction of the unreacted explosive)

$$\hat{n} = \frac{\vec{\nabla}\psi}{|\vec{\nabla}\psi|}. \tag{79}$$

The shock surface can be represented in terms of any valid surface parameterization that we choose, and we suppose that the shock surface can be represented by $\vec{x} = \vec{x}_s(\xi_1, \xi_2, t)$. The intrinsic coordinates are related to the laboratory coordinates by the change of variable given by

$$\vec{x} = \vec{x}_s(\xi_1, \xi_2, t) + n\,\hat{n}(\xi_1, \xi_2; t), \tag{80}$$

where the variables n, ξ_1, ξ_2 are respectively the distance measured in the direction of the normal to the shock wave, and the arclength measured in the directions defined by the principle normal curvatures at the shock surface.

If we travel in the shock surface in the direction of ξ_1 or ξ_2, we define the unit vectors of the local basis of this coordinate system in the shock surface (which are the tangent vectors to the coordinate directions), namely

$$\hat{t}_1 \equiv \frac{\partial \vec{x}_s}{\partial \xi_1}, \; \hat{t}_2 \equiv \frac{\partial \vec{x}_s}{\partial \xi_2}. \tag{81}$$

We restrict the remaining development to 2D to simplify the presentation.

5.2 Arc - length angle coordinates

Let ϕ measure an angle of the shock-attached normal to a fixed direction, here aligned in the z-direction (say). In the most general case, the reference direction can be a space curve with arbitrary orientation. We will refer to the reference space curve as the *edge*. The arclength in the surface is measured relative to the intersection of the shock surface with the reference curve, hence this intersection is the instantaneous origin for the intrinsic coordinate system. This definition of the origin allows for a unique mapping of the coordinates of the intrinsic coordinates to laboratory coordinates. In particular $n = 0$ always defines the shock surface, and $\xi = constant$ are space-time trajectories that measure constant arclength on the shock, relative to the edge.

At each point on the shock, the angle ϕ is defined so that the function $\phi(\xi, t)$ describes the orientation of the normals of the 2D shock. The normal and tangent unit vectors are defined in terms of the lab-coordinate basis vectors $\hat{e}_x, \hat{e}_z$ in the x and z-directions by

$$\hat{n} = sin(\phi)\hat{e}_x + cos(\phi)\hat{e}_z, \; \hat{t} = cos(\phi)\hat{e}_x - sin(\phi)\hat{e}_z. \tag{82}$$

The Frenet formulas applied to this coordinate system relate the derivatives of the unit vectors along the coordinate directions and reflect the fact that our coordinate system is locally orthogonal and is aligned along the lines of principle normal curvature. These formulas in 2D are

$$\frac{\partial \hat{t}}{\partial \xi} = -\kappa \hat{n}, \; \frac{\partial \hat{n}}{\partial \xi} = \kappa \hat{t}. \tag{83}$$

Notice that in 2D, the derivative of the angle ϕ, with respect to the arclength ξ defines the curvature κ

$$\kappa = \frac{\partial \phi}{\partial \xi}. \tag{84}$$

As an exercise the reader can check that according to the above formulas the basis of this intrinsic coordinate system is locally orthogonal, (i.e. the dot product of the normal and tangent vectors is zero).

The relation between the laboratory coordinate $\vec{x}$ and the arclength, angle coordinates is as follows. Since positions on the shock are described by

$$d\vec{x} = \hat{t} d\xi, \tag{85}$$

then it follows from the formula for $\hat{t}$ that

$$dx = cos(\phi) d\xi, \;\; dz = -sin(\phi) d\xi, \tag{86}$$

and integration of these formulas then obtains

$$x = x_e(t) + \int_0^{\xi} cos(\phi(\bar{\xi}, t)) d\bar{\xi}, \;\; z = z_e(t) - \int_0^{\xi} sin(\phi(\bar{\xi}, t)) d\bar{\xi}. \tag{87}$$

The coordinates of the edge, $x_e(t), z_e(t)$, are introduced for the purpose of measuring the arclength from a unique origin in the surface at each instant of time. These coordinates are found by locating the intersection of the edge and the shock surface and thus are necessarily functions of time. In general, the edge coordinates must be determined in the course of solving for the evolution of the shock.

5.3 Change of variable

The coordinate transformation implied by the definitions of the previous section change the representation of the governing equations that we have to solve. A change of variable is required to transform the equations into the n, ξ, t coordinates. In what follows, when a derivative is for fixed laboratory position, we will used the notation $|_{\vec{x}}$, and for fixed position in the shock attached coordinates, we will use $|_{\vec{\zeta}}$. In particular we must show how

$$\hat{e}_x, \hat{e}_z \text{ goes to } \hat{t}, \hat{n}, \tag{88}$$

$$\frac{\partial}{\partial x}, \frac{\partial}{\partial z} \text{ goes to } \frac{\partial}{\partial n}, \frac{\partial}{\partial \xi}, \tag{89}$$

and

$$\frac{\partial}{\partial t}_{|\vec{x}} \text{ goes to } \frac{\partial}{\partial t}_{|\vec{\zeta}}. \tag{90}$$

For example we need to compute the $\vec{\nabla}$ operator, which in the lab-fixed coordinates is written as

$$\vec{\nabla} \equiv \hat{e}_x \frac{\partial}{\partial x} + \hat{e}_z \frac{\partial}{\partial z}. \tag{91}$$

By the chain rule we have

$$\begin{aligned} \frac{\partial}{\partial x} &= \frac{\partial \xi}{\partial x}\frac{\partial}{\partial \xi} + \frac{\partial n}{\partial x}\frac{\partial}{\partial n}, \\ \frac{\partial}{\partial z} &= \frac{\partial \xi}{\partial z}\frac{\partial}{\partial \xi} + \frac{\partial n}{\partial z}\frac{\partial}{\partial n}, \end{aligned} \tag{92}$$

and we compute the derivatives $\xi_{,x}, \xi_{,z}, n_{,x}, n_{,z}$, from the coordinate transformation.

If we differentiate the coordinate transformation (in 2D)

$$x\hat{e}_x + z\hat{e}_z = \vec{x}_s(\xi, t) + n\hat{n}(\xi, t), \tag{93}$$

with respect to x and z respectively, and use the definition of $\hat{t}$ and the Frenet formulas (83), we obtain the following formulas

$$\hat{e}_x = \hat{t}\frac{\partial \xi}{\partial x} + \frac{\partial n}{\partial x}\hat{n} + n\kappa\frac{\partial \xi}{\partial x}\hat{t}, \tag{94}$$

$$\hat{e}_z = \hat{t}\frac{\partial \xi}{\partial z} + \frac{\partial n}{\partial z}\hat{n} + n\kappa\frac{\partial \xi}{\partial z}\hat{t}. \tag{95}$$

If we take the dot product of the above formulas with $\hat{n}$ and $\hat{t}$ respectively, we get the following relations for the direction cosines between the lab-fixed coordinates and the intrinsic coordinates

$$\hat{e}_x \cdot \hat{n} = \frac{\partial n}{\partial x}, \quad \hat{e}_x \cdot \hat{t} = (1 + n\kappa)\frac{\partial \xi}{\partial x},$$
$$\hat{e}_z \cdot \hat{n} = \frac{\partial n}{\partial z}, \quad \hat{e}_z \cdot \hat{t} = (1 + n\kappa)\frac{\partial \xi}{\partial z}. \tag{96}$$

The lab-fixed unit vectors, $\hat{e}_x, \hat{e}_z$ can be written in terms of their components in the intrinsic frame as

$$\hat{e}_x = (\hat{e}_x \cdot \hat{n})\hat{n} + (\hat{e}_x \cdot \hat{t})\hat{t},$$
$$\hat{e}_z = (\hat{e}_z \cdot \hat{n})\hat{n} + (\hat{e}_z \cdot \hat{t})\hat{t}. \tag{97}$$

The $\vec{\nabla}$ operator can then be written as

$$\vec{\nabla} = \left[(\hat{e}_x \cdot \hat{n})\hat{n} + (\hat{e}_x \cdot \hat{t})\hat{t}\right]\left(\frac{\partial \xi}{\partial x}\frac{\partial}{\partial \xi} + \frac{\partial n}{\partial x}\frac{\partial}{\partial n}\right) +$$
$$\left[(\hat{e}_z \cdot \hat{n})\hat{n} + (\hat{e}_z \cdot \hat{t})\hat{t}\right]\left(\frac{\partial \xi}{\partial z}\frac{\partial}{\partial \xi} + \frac{\partial n}{\partial z}\frac{\partial}{\partial n}\right). \tag{98}$$

If we multiply out the above result and use the properties of the unit vectors that $|\hat{t}| = |\hat{n}| = 1, \ \hat{t} \cdot \hat{n} = 0$, or

$$\left(\frac{\partial n}{\partial x}\right)^2 + \left(\frac{\partial n}{\partial z}\right)^2 = 1 \quad , \quad \left(\frac{\partial \xi}{\partial x}\right)^2 + \left(\frac{\partial \xi}{\partial z}\right)^2 = 1,$$
$$\frac{\partial n}{\partial x}\frac{\partial \xi}{\partial x} + \frac{\partial n}{\partial z}\frac{\partial \xi}{\partial z} = 0, \tag{99}$$

and use the fact that $\partial \hat{t}/\partial n = 0$, then the following formula results

$$\vec{\nabla} = \hat{t}\frac{1}{1 + n\kappa}\frac{\partial}{\partial \xi} + \hat{n}\frac{\partial}{\partial n}. \tag{100}$$

As another example, by using the definition of the velocity in the intrinsic coordinates

$$\vec{u} = u_\xi \hat{t} + u_n \hat{n}, \tag{101}$$

we calculate the divergence $\vec{\nabla} \cdot \vec{u}$, as

$$\vec{\nabla} \cdot \vec{u} = \frac{1}{1+n\kappa}\frac{\partial u_\xi}{\partial \xi} + \frac{\partial u_n}{\partial n} + \kappa\frac{u_n}{1+n\kappa} - \kappa u_\xi. \tag{102}$$

The time derivative in the lab-fixed coordinates is related to that in the shock-attached coordinates by the formula

$$\frac{\partial}{\partial t}|_{\vec{x}} = \frac{\partial}{\partial t}|_{\vec{\zeta}} + \frac{\partial n}{\partial t}|_{\vec{x}_\ell}\frac{\partial}{\partial n} + \frac{\partial \xi}{\partial t}|_{\vec{x}}\frac{\partial}{\partial \xi}, \tag{103}$$

where $\partial n/\partial t|_{\vec{x}} \equiv -D_n$ can be identified as the negative of the normal component of the shock surface velocity and, $\partial \xi/\partial t|_{\vec{x}} \equiv B$ is the instantaneous rate of increase or decrease of arclength along the shock. Thus we write

$$\frac{\partial}{\partial t}|_{\vec{x}} = \frac{\partial}{\partial t}|_{\vec{\zeta}} - D_n\frac{\partial}{\partial n} + B\frac{\partial}{\partial \xi}. \tag{104}$$

5.4 The governing equations in intrinsic coordinates

The governing equations in intrinsic coordinates follow from a straightforward application of the formulas of the previous section. We summarize them below: The equation of conservation of mass is given by

$$\frac{\partial \rho}{\partial t}|_{\vec{\zeta}} + \frac{\partial}{\partial n}(\rho(u_n - D_n)) + \kappa\frac{\rho u_n}{1+n\kappa} + \frac{1}{1+n\kappa}\frac{\partial(\rho u_\xi)}{\partial \xi} - \kappa\rho u_\xi + B\frac{\partial \rho}{\partial \xi} = 0. \tag{105}$$

The n-momentum equations is given by

$$\rho\left[\frac{\partial u_n}{\partial t} + (u_n - D_n)\frac{\partial u_n}{\partial n} + \frac{u_\xi}{1+n\kappa}\frac{\partial u_n}{\partial \xi} - u_\xi^2\frac{\kappa}{1+n\kappa} + B\frac{\partial u_n}{\partial \xi} - Bu_\xi\kappa\right] + \frac{\partial p}{\partial n} = 0. \tag{106}$$

The ξ-momentum equation is given by

$$\rho\left[\frac{\partial u_\xi}{\partial t} + (u_n - D_n)\frac{\partial u_\xi}{\partial n} + \frac{u_\xi}{1+n\kappa}\frac{\partial u_\xi}{\partial \xi} + u_\xi u_n\frac{\kappa}{1+n\kappa} + B\frac{\partial u_\xi}{\partial \xi} + Bu_n\kappa\right] + \frac{1}{1+n\kappa}\frac{\partial p}{\partial \xi} = 0. \tag{107}$$

The energy equation is given by

$$\frac{\partial e}{\partial t} + (u_n - D_n)\frac{\partial e}{\partial n} + \frac{u_\xi}{1+n\kappa}\frac{\partial e}{\partial \xi} + B\frac{\partial e}{\partial \xi}$$
$$-\frac{p}{\rho^2}\left[\frac{\partial \rho}{\partial t} + (u_n - D_n)\frac{\partial \rho}{\partial n} + \frac{u_\xi}{1+n\kappa}\frac{\partial \rho}{\partial \xi} + B\frac{\partial \rho}{\partial \xi}\right] = 0. \tag{108}$$

The rate equation is given by

$$\frac{\partial \lambda}{\partial t} + (u_n - D_n)\frac{\partial \lambda}{\partial n} + \frac{u_\xi}{1+n\kappa}\frac{\partial \lambda}{\partial \xi} + B\frac{\partial \lambda}{\partial \xi} = r. \tag{109}$$

5.5 Additional kinematics of the surface

In the equations of the last section the quantity

$$B \equiv \frac{\partial \xi}{\partial t}|_{\vec{x}}, \tag{110}$$

appears and represents the instantaneous change in the arclength along the shock. Here we give the derivation to show how this term is described completely in terms of quantities defined in the surface. By doing so, we derive the *kinematic surface relations.*

Differentiating the change of variable formula

$$\vec{x}_\ell = \vec{x}_s(\xi, t) + n\hat{n}(\xi, t), \tag{111}$$

with respect to t, holding $\vec{x}_\ell$ fixed (and using the chain rule and Frenet formulas) obtains,

$$0 = \frac{\partial \vec{x}_s}{\partial t}|_{\zeta} + \hat{t}\frac{\partial \xi}{\partial t}|_{\vec{x}} + \frac{\partial n}{\partial t}|_{\vec{x}}\hat{n} + n\left\{\frac{\partial \hat{n}}{\partial t}|_{\zeta} + \kappa\hat{t}\frac{\partial \xi}{\partial t}|_{\vec{x}}\right\}. \tag{112}$$

We specialize this result to the surface $\vec{x} = \vec{x}_s$, set $n = 0$, and use the definition $\partial\vec{x}_s/\partial\xi = \hat{t}$ and $\partial n/\partial t|_{\vec{x}} = -D_n$ to obtain

$$\frac{\partial \vec{x}_s}{\partial t}|_{\zeta} + \hat{t}\frac{\partial \xi}{\partial t}|_{\vec{x}_s} - D_n\hat{n} = 0. \tag{113}$$

Next we differentiate (113) with respect to ξ, holding t fixed, and use the Frenet formulas to obtain the following vector equation that describes the kinematics in the shock surface

$$\frac{\partial \hat{t}}{\partial t}|_{\xi} + \frac{\partial}{\partial \xi}\left(\frac{\partial \xi}{\partial t}|_{\vec{x}_s}\right)\hat{t} - \kappa \frac{\partial \xi}{\partial t}|_{\vec{x}_s}\hat{n} - \frac{\partial D_n}{\partial \xi}\hat{n} - D_n \kappa \hat{t} = 0. \tag{114}$$

We dot the last equation with $\hat{n}$ to obtain the n- component and obtain

$$\hat{n} \cdot \frac{\partial \hat{t}}{\partial t}|_{\xi} - \kappa \frac{\partial \xi}{\partial t}|_{\vec{x}_s} - \frac{\partial D_n}{\partial \xi} = 0, \tag{115}$$

and dot the same equation by $\hat{t}$ to obtain the ξ - component as

$$\frac{\partial}{\partial \xi}\left(\frac{\partial \xi}{\partial t}|_{\vec{x}_s}\right) - D_n \kappa = 0. \tag{116}$$

This pair of surface relations can be used to describe the shock surface evolution solely in terms of angle - arclength coordinates as follows. From the formulas that define the normal and tangent vector in terms of the shock normal reference angle ϕ, (82), and the definition of the plane curvature, (84), we find that

$$\frac{\partial \hat{t}}{\partial t}|_{\xi} = -\hat{n}\frac{\partial \phi}{\partial t}|_{\xi}\,. \tag{117}$$

By integrating equation (116) with respect to ξ, and using the definition $\kappa = \partial \phi / \partial \xi$, we get the explicit expression for the instantaneous rate of change of the arc length,

$$B \equiv \frac{\partial \xi}{\partial t}|_{\vec{x}} = \int_0^{\xi} D_n \frac{\partial \phi}{\partial \xi} d\bar{\xi} + f(t). \tag{118}$$

where $f(t)$ is an integration constant. Finally from the $D_n - \kappa$ relation, we have the fact that $D_n(\kappa)$ is presumed to be a known function. Substituting these results back into (116) yields the intrinsic, integro-differential equation, for $\phi(\xi, t)$.

$$\frac{\partial \phi}{\partial t} + B\frac{\partial \phi}{\partial \xi} = \frac{dD_n(\kappa)}{d\kappa}\frac{\partial^2 \phi}{\partial \xi^2}. \tag{119}$$

This equation was derived first in [16] by a different route.

Importantly, the results of this section can be used to make explicit estimates of the asymptotic orders of certain dynamic terms that occur in the governing equations. We explore this in the next section.

6 Asymptotic Scaling

Recall the basic results that we had previously obtained by discussing Cartesian coordinates where the shock locus was given by

$$\psi = z - D_{CJ}t - z_s(x,t) = 0. \tag{120}$$

The normal detonation velocity was given by

$$D_n = \frac{D_{CJ} + \partial z_s/\partial t}{[1 + (\partial z_s/\partial x)^2]^{1/2}}, \tag{121}$$

and the plane curvature was given by

$$\kappa = \frac{\partial^2 z_s}{\partial x^2} \frac{1}{[1 + (\partial z_s/\partial x)^2]^{3/2}}. \tag{122}$$

Also recall that the steady ZND, 1/2-reaction zone length was given by the integral

$$\ell_{rz} = \int_{\lambda=0}^{\lambda=1/2} \frac{U_*(\bar{\lambda})}{r(p_*(\bar{\lambda}, \rho_*(\bar{\lambda}), \bar{\lambda})} d\bar{\lambda}, \tag{123}$$

where the * subscript refers to quantities defined by the steady state.

In what follows, within this section, we adopt the notation convention where a quantity with a $\tilde{()}$ refers to a dimensional quantity and the quantities without a tilde are dimensionless quantities that are scaled with respect to the dimensional unit. In particular we choose the following scales for length, velocity and time

$$\begin{aligned} \text{length} &\quad - \quad \tilde{\ell}_{rz}, \\ \text{velocity} &\quad - \quad \tilde{D}_{CJ}, \\ \text{time} &\quad - \quad \tilde{\ell}_{rz}/\tilde{D}_{CJ}. \end{aligned} \tag{124}$$

Then the formulas (in Cartesian coordinates) for the normal detonation velocity and the curvature become

$$D_n = \frac{\tilde{D}_n}{\tilde{D}_{CJ}} = \frac{1 + \partial z_s/\partial t}{[1 + (\partial z_s/\partial x)^2]^{1/2}}, \tag{125}$$

and

$$\kappa \equiv \tilde{\kappa}\tilde{\ell}_{rz} = \frac{\partial^2 z_s/\partial x^2}{[1 + (\partial z_s/\partial x)^2]^{3/2}}. \tag{126}$$

Recall the limit of small shock slope, can be expressed as

$$\frac{\partial z_s}{\partial x} \approx O(\epsilon). \tag{127}$$

The reaction zone thickness is now the basic, O(1), unit of distance measurement in our theory. The natural way to express slow variations along the shock, measured in a direction transverse to the shock, is to introduce the slowly varying length scale

$$X = \epsilon x. \tag{128}$$

Transverse variations are measured on the $X \sim O(1)$ length scale so that when $\partial/\partial X \sim O(1)$ then $\partial/\partial x = \epsilon \partial/\partial X \sim O(\epsilon)$.
It follows that the shock slope scales as

$$\frac{\partial z_s}{\partial x} \approx \epsilon \frac{\partial z_s}{\partial X}. \tag{129}$$

The argument that we had used in section 3.5, suggests that if temporal changes in the movement of the detonation shock are to affect the detonation velocity at the same order as the shape changes, then the relevant time scale must be such that

$$\frac{\partial z_s}{\partial t} \sim O(\epsilon^2), \text{ since } \left(\frac{\partial z_s}{\partial x}\right)^2 \sim O(\epsilon^2). \tag{130}$$

Thus we introduce the slow time variations and introduce the time scale

$$\tau = \epsilon^2 t, \tag{131}$$

so that

$$\frac{\partial}{\partial t} = \epsilon^2 \frac{\partial}{\partial \tau}. \tag{132}$$

6.1 The expansion procedure

What follows next is a discussion of the expansion procedure that is used to derive a reduced set of equations that will describe the quasi-steady, weakly curved dynamics of near-CJ detonation shocks. The smallness of the shock curvature is measured relative to the to the reaction zone thickness in the normal direction.

There are two main developments that must be in place before we can start this reduction, and they have been covered in the previous sections: i) The governing equations need to be written in a shock-attached frame. ii) Scaling assumptions that describe the nature of the unsteadiness and their relation to the shape changes of the shock must be adopted. The scaling assumptions are those associated with a particular asymptotic distinguished limit of the reactive, multidimensional Euler equations. The multi-scale asymptotic expansions that are described next (although perhaps robust in their ability to model the underlying physical system) are mathematically restricted to describe the shock dynamics within the limits of the scaling assumptions and following expansions.

The expansions that we list here are motivated by the dynamics implicit in the shock relations and the fact that to leading order, we expect the detonation to behave in a quasi-steady fashion. We reintroduce dimensional equations here, and temporarily retain ϵ as the small parameter that describes the small relative curvature. The variable n still measures distance in the shock normal direction and is negative within the reaction zone and zero at the shock. We retain τ as the relevant time scale, and use ζ as the slow transverse spatial scale that measures arclength along the shock, defined by

$$\zeta = \epsilon \xi. \tag{133}$$

The expansions of the dependent variables for the simplest version of DSD-theory are

$$u_\xi = \epsilon u_\xi^{(1)}(n) + o(\epsilon),$$

$$
\begin{aligned}
u_n &= u_n^{(0)}(n) + \epsilon^2 u_n^{(2)}(n,\zeta,\tau) + o(\epsilon^2), \\
\rho &= \rho^{(0)}(n) + \epsilon^2 \rho^{(2)}(n,\zeta,\tau) + o(\epsilon^2), \\
p &= p^{(0)}(n) + \epsilon^2 p^{(2)}(n,\zeta,\tau) + o(\epsilon^2), \\
\lambda &= \lambda^{(0)}(n,\tau) + \epsilon^2 \lambda^{(0)}(n,\zeta,\tau) + o(\epsilon^2).
\end{aligned} \tag{134}
$$

In addition to the dependent variable, we also expand the normal detonation velocity (in the simplest version of the theory) in terms of the shock curvature as

$$
D_n = 1 + \epsilon^2 D_n^{(2)}(\zeta,\tau) + \dots, \tag{135}
$$

where κ is related to ϵ by

$$
\kappa = \epsilon^2 \kappa^{(2)}. \tag{136}
$$

Note by assuming the expansions (135) and (136) we have assumed that the leading order correction to the normal detonation velocity is $O(\kappa)$. This assumption is verified if the analysis determines the coefficient $D_n^{(2)}$, and is correct for the simplest case presented here. However in general the leading order correction to D_n can have a different dependence on κ. For example, in [5] and [8] it is shown that the leading correction to D_n is $O(\kappa \ln \kappa)$ for a rate of the form $r = k(p,\rho)(1-\lambda)$.

The $O(1)$ terms in the expansions for u_n, ρ, p and λ, reflect the steady, 1D, ZND, solution in the shock-attached coordinates. The full expansions for the dependent variables, the curvature and the detonation velocity are substituted into the governing equations (105) - (109). This leads to, in the standard way, a hierarchy of systems of equations at O(1), $O(\epsilon)$, and $O(\epsilon^2)$. Each set of equations must then be solved in a consistent manner to ultimately produce a uniform approximation within the space and time domain of interest.

While this procedure is general and precise, we replace it with a simple and entirely equivalent procedure, whereby we analyze each term in the governing equations, using estimates in terms of ϵ that are found in the expansions (136) and from the scaling definitions. We then discard terms that are smaller than $O(\epsilon^2)$, i.e. below the order of the curvature. This analysis was carried out systematically in [8], however Whitham's shock ray coordinates are used rather than the Bertrand coordinates that appear in these notes. What follows is a discussion that analysis and we go through the governing equations, essentially term by term. We discuss the negligible terms in detail.

Starting with the unsteady term in (105), we get the estimate

$$\frac{\partial \rho}{\partial t}|_{\vec{\zeta}} = O(\epsilon^4). \tag{137}$$

This estimate follows from two facts, that the leading order approximation $\rho^{(0)}$ is assumed not to depend on τ and that the next correction to ρ is $O(\epsilon^2)$.

The term

$$\frac{1}{1+n\kappa}\frac{\partial}{\partial \xi}(\rho u_\xi) = o(\epsilon^2), \tag{138}$$

because we have slow transverse variations and u_ξ is assumed to be $O(\epsilon)$ and not to depend explicitly on ζ. The term

$$\kappa u_\xi = O(\epsilon^3). \tag{139}$$

The term in the mass conservation equation is

$$B\frac{\partial \rho}{\partial \xi} = O(\epsilon^4), \tag{140}$$

and to show this, we need to invoke an estimate of $B = \partial\xi/\partial t|_{\vec{x}}$.

Recall from (116) that B must satisfy the kinematic surface relation

$$\frac{\partial B}{\partial \xi} = D_n \kappa, \tag{141}$$

so that in order to be consistent,

$$B = \frac{\partial \xi}{\partial t}|_{\vec{x}} \sim O(\epsilon). \tag{142}$$

A list of other negligible terms and their estimates obtained by similar arguments is found below. In the n-momentum equation we find

$$\frac{\partial u_n}{\partial t}|_{\vec{\zeta}} = O(\epsilon^4),\ \frac{u_\xi}{1+n\kappa}\frac{\partial u_n}{\partial \xi} = O(\epsilon^4),$$
$$\frac{u_\xi^2\kappa}{1+n\kappa} = O(\epsilon^4),\ B\frac{\partial u_n}{\partial \xi} = O(\epsilon^4),\ Bu_\xi\kappa = O(\epsilon^4). \tag{143}$$

The estimates of negligible terms in the ξ- momentum equation are

$$\frac{\partial u_\xi}{\partial t}|_{\vec{\zeta}} = O(\epsilon^3), \quad \frac{u_\xi}{1+n\kappa}\frac{\partial u_\xi}{\partial \xi} = O(\epsilon^4),$$

$$\frac{u_\xi u_n \kappa}{1+n\kappa} = O(\epsilon^3), \; B\frac{\partial u_\xi}{\partial \xi} = O(\epsilon^3), \; B u_n \kappa = O(\epsilon^3). \tag{144}$$

In the rate equation we neglect

$$\frac{\partial \lambda}{\partial t}|_{\vec{\zeta}} = O(\epsilon^4), \quad \frac{u_\xi}{1+n\kappa}\frac{\partial \lambda}{\partial \xi} = O(\epsilon^4), \; B\frac{\partial \lambda}{\partial \xi} = O(\epsilon^4). \tag{145}$$

From the ξ-momentum equation we find the following, simple result. From the $O(\epsilon)$ equation we find that $u_\xi^{(1)}$ obeys

$$\frac{\partial u_\xi^{(1)}}{\partial n} = 0. \tag{146}$$

Integrating this equation shows,

$$u_\xi^{(1)} = f(\xi, \tau). \tag{147}$$

But since the normal shock relations show that there is no jump in u_ξ across the shock, combined with the assumption that the upstream state is quiescent, shows that

$$u_\xi^{(1)} = 0, \quad \text{for all } \zeta \text{ and } \tau. \tag{148}$$

Consequently we find that

$$u_\xi = o(\epsilon), \tag{149}$$

and some of the estimates of this section that involve u_ξ can be further refined.

7 The Reduced Problem for $D_n - \kappa$

If we retain only the terms in (105) - (109) that may contribute terms up to order $O(\epsilon^2) \sim \kappa$, we find the reduced set

$$\frac{\partial}{\partial n}(\rho(u_n - D_n)) + \rho u_n \kappa = 0, \tag{150}$$

$$\rho(u_n - D_n)\frac{\partial u_n}{\partial n} + \frac{\partial p}{\partial n} = 0, \tag{151}$$

$$\frac{\partial e}{\partial n} - \frac{p}{\rho^2}\frac{\partial \rho}{\partial n} = 0, \tag{152}$$

$$(u_n - D_n)\frac{\partial \lambda}{\partial n} = r. \tag{153}$$

In addition to these equation we add the (strong) shock relations at the location $n = 0$, which we reproduce here for convenience

$$\begin{aligned} \rho_s &= \rho\frac{\gamma+1}{\gamma-1}, & p_s &= \frac{2}{\gamma+1}\rho_0 D_n^2, \\ U_n = u_n - D_n &= -D_n\frac{\gamma-1}{\gamma+1}, & u_\xi &= 0, \ \ \lambda_s = 0. \end{aligned} \tag{154}$$

The shock relations essentially serve as boundary conditions for fixed D_n.

As part of the general formulation, a total integral of the energy can be obtained from combinations of the above differential equations. This relation is essentially Bernoulli's equation for the total energy on a streamtube, where the value of the total energy integral is evaluated at the shock. The strong shock result is given by

$$e(p, \rho, \lambda) + \frac{p}{\rho} + \frac{(u_n - D_n)^2}{2} = \frac{D_n^2}{2}. \tag{155}$$

7.1 Derivation of the master equation

In this section, we give a derivation of the master equation for the general $e(p, v, \lambda)$ equation of state, and then take the special case of the polytropic equation of state. We start with an arbitrary EOS to obtain

$$\frac{\partial e}{\partial \rho}\frac{\partial \rho}{\partial n} + \frac{\partial e}{\partial p}\frac{\partial p}{\partial n} + \frac{\partial e}{\partial \lambda}\frac{\partial \lambda}{\partial n} - \frac{p}{\rho^2}\frac{\partial \rho}{\partial n} = 0, \tag{156}$$

Which we rewrite as

$$-\frac{[p/\rho^2 - \partial e/\partial \rho]}{\partial e/\partial p}\frac{\partial \rho}{\partial n} + \frac{\partial p}{\partial n} + \frac{\partial e/\partial \lambda}{\partial e/\partial p}\frac{\partial \lambda}{\partial n} = 0. \tag{157}$$

We note the general definition of the frozen sound speed as

$$c^2 \equiv \frac{[p/\rho^2 - \partial e/\partial \rho]}{\partial e/\partial p}, \tag{158}$$

so that the previous result can also be written as

$$-c^2\frac{\partial \rho}{\partial n} + \frac{\partial p}{\partial n} + \frac{\partial e/\partial \lambda}{\partial e/\partial p}\left(\frac{\partial \lambda}{\partial n}\right) = 0. \tag{159}$$

The next step is to eliminate the pressure p and the density ρ in favor of the relative velocity $U_n \equiv u_n - D_n$ and the mass fraction λ. From the momentum equation we find that

$$\frac{\partial p}{\partial n} = -\rho U_n \frac{\partial U_n}{\partial n}, \tag{160}$$

and from the mass conservation equation we find that

$$\frac{\partial \rho}{\partial n} = -\rho\kappa\frac{U_n + D_n}{U_n} - \frac{\rho}{U_n}\frac{\partial U_n}{\partial n}. \tag{161}$$

These two substitutions are then used in the energy equation and results in an equation that is quasi-linear in U_n and λ. If we use λ as independent variable instead of n, the rate equation provides the replacement

$$\frac{\partial}{\partial n} = \frac{r}{U_n}\frac{\partial}{\partial \lambda}. \tag{162}$$

By replacing the derivative $\partial/\partial n$ in the quasi-linear form of the energy equation by $\partial/\partial\lambda$ and replacing $\partial\lambda/\partial n$ by r/U_n and then solving for $\partial U_n/\partial\lambda$, we obtain an equation that determines U_n as a function of λ

$$\frac{\partial U_n}{\partial \lambda} = -U_n \frac{\left[c^2\rho(U_n + D_n)\kappa + \frac{1}{\rho}\frac{\partial e/\partial \lambda}{\partial e/\partial p}r\right]}{r[c^2 - U_n^2]}. \tag{163}$$

7.2 The special case of the ideal EOS

Now we turn to an example of the ideal equation of state. This choice has the advantage that much of the theory has a simpler form, and that there is a large body of established theory and numerics. The ideal (or polytropic) EOS is given by

$$e = \frac{p}{\rho}\frac{1}{\gamma - 1} - Q\lambda. \tag{164}$$

Then some of the thermodynamic quantities in the expressions of the previous section are

$$\frac{1}{\rho}\frac{\partial e/\partial\lambda}{\partial e/\partial p} = -Q(\gamma - 1), \tag{165}$$

$$c^2 = \gamma\frac{p}{\rho}. \tag{166}$$

By using the total energy equation we can get an expression for c^2 that only depends on U_n and λ as

$$c^2 = \frac{\gamma - 1}{2}(D_n^2 - U_n^2) + Q(\gamma - 1)\lambda. \tag{167}$$

The master equation can then be written in the form

$$\frac{\partial U_n}{\partial\lambda} = \frac{U_n\Phi}{r\eta}, \tag{168}$$

where

$$\Phi \equiv (\gamma - 1)Qr - c^2(U_n + D_n)\kappa, \tag{169}$$

and

$$\eta \equiv c^2 - U_n^2. \tag{170}$$

A rate law with simple depletion that has a premultiplying rate constant that is sound speed (temperature) dependent is generally of the form

$$r = k(c^2)(1 - \lambda)^{\nu}. \tag{171}$$

7.3 The shooting problem for the $D_n - \kappa$ relation.

Here we discuss the shooting problem that determines the $D_n - \kappa$ relation. Note that the sign convention we have used assumes that when the detonation shock is convex, relative to the ambient flow, that the curvature is positive. This is the case of a diverging detonation.

The master equation (163) was derived for an arbitrary EOS of the form $e(p, \rho, \lambda)$, and has the general form

$$\frac{\partial U_n}{\partial \lambda} = \frac{U_n \Phi}{r\eta}, \tag{172}$$

where

$$\Phi = -\frac{1}{\rho}\frac{\partial e/\partial \lambda}{\partial e/\partial \rho} - c^2(U_n + D_n)\kappa, \tag{173}$$

and η is defined by (170). The solution to the master equation can be entirely described in a $U_n - \lambda$ plane if the right hand side of (172) can be written entirely as a function of at most U_n and λ. If this is not the case, and for example, the density dependence cannot be eliminated explicitly from (172), then the continuity equation must be added for a complete description.

For the shooting problem, for general EOS, one must also solve the shock relations to obtain a boundary condition of the form

$$U_n = U_n(D_n) \text{ at } \lambda = 0. \tag{174}$$

The integral curve must start at the shock, with $\lambda = 0$ and for positive curvature pass through a singular point that corresponds to a condition where the flow becomes sonic (i.e. $\eta = 0$). So that we have a nonsingular solution at the sonic point, the integral curve must be such that Φ and η simultaneously vanishes there. The condition that the $U_n - \lambda$ integral curve pass through the point in the $U_n - \lambda$ plane defined by the conditions

$$\Phi = 0 \text{ and } \eta = 0, \tag{175}$$

is called the *generalized CJ condition* after Wood and Kirkwood, [3], and must be applied in addition to the shock boundary condition. The task of solving for an integral curve in the $U_n - \lambda$ plane is overdetermined unless one allows for a relation between D_n and κ.

The master equation (163) subject to the shock boundary condition (174) and the generalized CJ condition, is a self-contained problem, providing that it is possible to write the thermodynamic quantities, c^2, $(\partial e/\partial\lambda)/(\rho\,\partial e/\partial p)$ and the rate law r, solely in terms of U_n and λ. This cannot be always be done for a non-ideal equation of state or rate law. Rather it is true only under some special circumstances, like the example shown in section 7.2 for the ideal equation of state, and a rate law which had a rate premultiplier that is only function of c^2.

Once the integral curve $U_n(\lambda)$ is found, one can recover the density and the pressure from the integration of

$$\frac{r}{U_n}\frac{\partial(\rho U_n)}{\partial\lambda} = -\rho(U_n + D_n)\kappa, \tag{176}$$

and

$$\frac{\partial p}{\partial\lambda} = -\rho U_n \frac{\partial U_n}{\partial\lambda}. \tag{177}$$

subject to the appropriate shock conditions. The spatial structure of the reaction zone is then finally determined by

$$n = \int_0^\lambda \frac{U_n}{r} d\lambda. \tag{178}$$

7.4 The shooting problem for general EOS

The general formulation of the shooting problem requires the the simultaneous integration of either the mass or momentum equations, in addition to the master equation to describe the solution through the reaction zone. The general formulation (for one reaction variable) can be written in terms of two coupled nonautonomous equations for either (ρ, P), (ρ, U_n)or (U_n, P). The missing dependent variable is supplied through the total energy integral,

$$e(p,\rho,\lambda) + \frac{p}{\rho} + \frac{U_n^2}{2} = e(p_s,\rho_s,0) + \frac{D_n^2}{2} + \frac{p_s}{\rho_s}. \tag{179}$$

The relevant equations for ρ, U_n and p, with λ as the independent variable are

$$\frac{\partial \rho}{\partial \lambda} = -\frac{\rho}{r}\left[(U_n + D_n)\kappa + \frac{\Phi}{\eta}\right], \tag{180}$$

$$\frac{\partial U_n}{\partial \lambda} = \frac{U_n \Phi}{r\eta}, \tag{181}$$

$$\frac{\partial p}{\partial \lambda} = -\frac{\rho U_n^2 \Phi}{r\eta}. \tag{182}$$

A numerical procedure is a robust way to determine the determine the solution and the $D_n - \kappa$ relation. A successful iterative procedure starts the integration of the ODEs at the shock, and integrates toward the end of the reaction zone. For a fixed D_n, κ pair, one of the two of the generalized CJ conditions will be satisfied first, while the other is not. One uses the residual, i.e. the nonzero value of the condition, to develop an iteration procedure (like a Newton-Raphson or secant method) to change D_n (say) systematically. The integration is repeated until the shock conditions and the generalized CJ conditions are satisfied simultaneously. Lee, Persson and Bdzil used this procedure recently to determine both the $D_n - \kappa$ relation and the rate law for nonideal, ammonium nitrate-based explosive used in mining applications, [13].

8 The Singular Perturbation Solution to the $D_n - \kappa$ Relation for Ideal EOS

More extensive discussions of the analysis presented here are found in [5], and in particular [8].

We reintroduce the dimensional scales so that the resulting problem that we finally analyze is dimensionless. The following quantities and parameters are defined for the ideal equation of state described in section 7.2,

$$\begin{aligned} U_n &= \tilde{U}_n/\tilde{D}_{CJ}, \qquad c = \tilde{c}/\tilde{D}_{CJ}, \;\; r = \tilde{r}\tilde{\ell}_{rz}/\tilde{D}_{CJ} \\ D_n &= \tilde{D}_n/\tilde{D}_{CJ}, \qquad \kappa = \tilde{\kappa}\tilde{l}_{rz}, \;\; q = \tilde{Q}/\tilde{D}_{CJ}^2. \end{aligned} \tag{183}$$

Having done this we obtain the dimensionless version of the master equation for an ideal equation of state and idealized rate law as

$$\frac{\partial U_n}{\partial \lambda} = U_n \frac{[(\gamma-1)qr - c^2(U_n + D_n)\kappa]}{r(c^2 - U_n^2)}, \tag{184}$$

where c^2 in terms of U_n and λ is given by

$$c^2 = \frac{\gamma - 1}{2}(D_n^2 - U_n^2) + q\lambda(\gamma - 1), \tag{185}$$

with the shock condition

$$U_n = -\frac{\gamma - 1}{\gamma + 1} D_n. \tag{186}$$

To illustrate the theory we will treat the simplest case where k in (171) is a constant and is not state-dependent.

The objective here is to describe the asymptotic solution to this problem in the limit as $\kappa \to 0$. The solution is an integral curve in the $U_n - \lambda$ - plane that starts from the shock and ends up at the generalized CJ point.

8.1 Location of the critical point in the $U_n - \lambda$ - plane

The location of the generalized CJ-point is given by the conditions

$$\Phi = 0, \quad \text{and} \quad \eta = 0. \tag{187}$$

These conditions respectively are

$$(\gamma - 1)qk(1 - \lambda)^\nu = c^2(U_n + D)\kappa, \tag{188}$$

and

$$c^2 = U_n^2. \tag{189}$$

In particular, in equation (188), as $\kappa \to 0$, we must have $\lambda \to 1$, so that we can make the assumptions near the generalized CJ point,

$$D_n = 1 + D_n' + \ldots, \quad \lambda = 1 - \lambda' + \ldots. \tag{190}$$

Substitution of those expansion into the previous expression gives approximate expressions

$$\lambda' = \left(\frac{2\gamma^2}{(\gamma+1)^2 k}\right)^{1/\nu} \kappa^{1/\nu}, \tag{191}$$

and

$$U_n^2 = \frac{\gamma^2}{(\gamma+1)^2} + 2\frac{\gamma-1}{\gamma+1} D_n' - \frac{1}{(\gamma-1)^2}\lambda' + \ldots. \tag{192}$$

We obtain two algebraic conditions from this analysis near the singular point. Notice that the order of D_n' is not determined by this analysis.

8.2 Near-shock expansion

The analysis of the structure of the solution to this problem breaks into two pieces, in the spirit of layer analysis of singular perturbation theory. There is generally a near-shock layer and a layer near the generalized CJ point. In these notes we will treat the simplest case possible, when the relationship between D_n and κ is linear.

We suppose that the near-shock layer has a regular perturbation expansion in terms of κ of the form

$$U_n = U^{(0)}(\lambda) + \kappa U^{(1)}(\lambda) + \ldots, \tag{193}$$

and represent D_n by

$$D_n = 1 + \kappa D_n^{(1)} + \ldots. \tag{194}$$

The object of the analysis is to find a formula for $D_n^{(1)}$. Substitution of the above expansions into (184) and (186) and collecting powers of κ gives the problems for $U^{(0)}, U^{(1)}$. At $O(1)$ we obtain

$$((c^{(0)})^2 - (U^{(0)})^2)\frac{\partial U^{(0)}}{\partial \lambda} = U^{(0)}(\gamma-1)q, \tag{195}$$

subject to the shock boundary condition

$$U^{(0)} = -\frac{\gamma-1}{\gamma+1} \quad \text{at} \quad \lambda = 0, \tag{196}$$

where $(c^{(0)})^2$ is determined in terms of $U^{(0)}$ and λ from (185).

At $O(\kappa)$ we have

$$\begin{aligned}((c^2)^{(1)} - (U^2)^{(1)})\frac{\partial U^{(0)}}{\partial \lambda} &+ ((c^{(0)})^2 - (U^{(0)})^2)\frac{\partial U^{(1)}}{\partial \lambda} = \\ U^{(1)}q(\gamma - 1) &- U^{(0)}(c^{(0)})^2(U^{(0)} + 1)/r^{(0)},\end{aligned} \tag{197}$$

(where $r^{(0)} = k(1-\lambda)^\nu$), and $U^{(1)}$ is subject to

$$U^{(1)} = -\frac{\gamma - 1}{\gamma + 1}D_n^{(1)} \text{ at } \lambda = 0. \tag{198}$$

Note that $(c^2)^{(1)}$ is also determined from (185) in terms of $U^{(1)}, U^{(0)}$ and λ, and $(U^2)^{(1)} = 2U^{(0)}U^{(1)}$. For convenience we introduce the variable

$$\ell \equiv \sqrt{1 - \lambda}. \tag{199}$$

Both of the problems listed above can be solved explicitly.

The $O(1)$ problem is exactly the same as the 1D, steady, CJ, ZND detonation wave, see section 4.3.1. The $O(1)$ problem requires the solution of a separable first order ODE and the solution is given by

$$U^{(0)} = -\frac{\gamma - \ell}{\gamma + 1}. \tag{200}$$

The solution to the $O(\kappa)$ equation for $U^{(1)}$ is

$$U^{(1)} = -\frac{D_n^{(1)}}{\gamma + 1}\left(\gamma - \frac{1}{\ell}\right) - \frac{1}{\gamma + 1}\left(\frac{1}{\gamma} - \frac{1}{\ell}\right)\int_\ell^1 F(\hat{\ell})d\hat{\ell}, \tag{201}$$

where $F(\ell)$ is defined by

$$F(\ell) = \frac{2\gamma^2}{(\gamma + 1)^2}\frac{(1 + \ell)^2\ell^{1-2\nu}}{k}. \tag{202}$$

At this point the leading order correction to the $D_n - \kappa$ relation can be derived by using the principal of elimination of the strongest singularity. In this case, a singularity exists in the $O(\kappa)$ expansion and must be removed to obtain a regular solution near the end of the reaction zone.

Note that in the near-shock expansion that the solution for $U^{(1)}$ becomes singular at the tail of the reaction zone as $\lambda \to 1$, i.e. as $\ell \to 0$, $U^{(1)}$, without further assumption would become asymptotic to $O(1/\ell)$. Thus sufficiently close to the end of the reaction zone the expansion becomes nonuniform. The simplest argument that can be made is that this nonuniformity is not a characteristic of the physical solution and it is not present in the physical flow. We can eliminate the nonuniformity by choosing $D_n^{(1)}$ according to the formula

$$D_n^{(1)} = -\int_0^1 F(\hat{\ell})d\hat{\ell}. \tag{203}$$

With this choice the solution for $U^{(1)}$ becomes

$$\begin{aligned} U^{(1)} = \frac{\gamma}{\gamma+1}\int_0^1 F(\hat{\ell})d\hat{\ell} \quad &- \quad \frac{1}{\gamma(\gamma+1)}\int_\ell^1 F(\hat{\ell})d\hat{\ell} \\ &+ \quad \frac{1}{\ell(\gamma+1)}\int_\ell^0 F(\hat{\ell})d\hat{\ell}, \end{aligned} \tag{204}$$

and this solution is not singular as $\ell \to 0$ since $\int_\ell^0 F(\hat{\ell})d\hat{\ell} \sim \ell$.

Notice also that the integral that defines $D_n^{(1)}$ depends on the form of the rate law and the equation of state. For this choice of the rate law made here, the integral is convergent only for values of $0 \leq \nu < 1$. For $\nu = 1$, the integral is formally divergent, which indicates that the leading order correction to D_n is not $O(\kappa)$, but is larger. (It turns out that for $\nu = 1$ the leading order correction is $O(\kappa\, ln(\kappa))$, [5], [8].)

8.3 The transonic layer

Here we give the results in the transonic layer, near the end of the reaction zone. Note that we make an expansion where the values of U and λ are assumed to be close to the values determined from the generalized CJ conditions. Recall that the values of their were determined to leading order according to

$$\begin{aligned} 1-\lambda = (z_*)^{1/\nu}\kappa^{1/\nu}, \quad &\text{where } z_* = \frac{2\gamma^2}{(\gamma+1)^2 k} \\ \text{and } U_n = \frac{\gamma}{\gamma+1} + &\frac{\gamma-1}{\gamma}[D_n' - 2q(z_*)^{1/\nu}\kappa^{1/\nu}], \end{aligned} \tag{205}$$

where D_n' is the general form perturbation of the detonation velocity, with out its order specified.

What form does the expansion of U take in this layer? The question can be answered by looking at the leading order of the outer solution (the near-shock solution) and evaluating it at the generalized CJ point. Note that if we do that formally, we get

$$U^{(0)} = -\frac{\gamma}{\gamma+1} + \frac{(z_*\kappa)^{1/2\nu}}{\gamma+1}. \tag{206}$$

This simple result strongly suggests the form on the TSL expansion must take. We introduce the new layer coordinate

$$(z_*\kappa)^{1/\nu} s = (1-\lambda). \tag{207}$$

Notice that the term $\kappa^{1/\nu}$ appears explicitly.

We write the expansion in the TSL as

$$U_n^{TSL} = -\frac{\gamma}{\gamma+1} + (z_*\kappa)^{1/2\nu} u^{(1/2\nu)}(s) + \dots . \tag{208}$$

The governing equation for $u^{(1/2\nu)}$ derived from the master equation is

$$\frac{\partial (u^{(1/2\nu)})^2}{\partial s} = \frac{1}{(\gamma+1)^2}\left(1 - \frac{1}{s^\nu}\right), \tag{209}$$

subject to the boundary condition

$$u^{(1/2\nu)} = 0 \ \text{ at } \ s = 0. \tag{210}$$

The solution to the above problem is

$$u^{(1/2\nu)} = \frac{1}{\gamma+1}\left[s - 1 - \frac{s^{1-\nu}-1}{1-\nu}\right]^{1/2}. \tag{211}$$

The TSL solution is given by

$$U_n^{TSL} = -\frac{\gamma}{\gamma+1} + (z_*)^{1/2\nu}\frac{1}{\gamma+1}\left[s - 1 - \frac{s^{1-\nu}-1}{1-\nu}\right]^{1/2} \kappa^{1/2\nu}. \tag{212}$$

8.4 Summary

In summary, we have solved for the solution through the reaction zone and obtained the leading order corrections that are $O(\kappa)$ and have found that the solution is split into two regions, a near-shock layer (called the main reaction layer MRL) and a near-sonic region, near complete reaction (the transonic layer TSL). Importantly, in order for the solutions to match, and so that we obtain a uniformly valid description, we must have an eigenvalue relationship between the perturbation of the detonation velocity. When we carry out an expansion using the curvature as our perturbation parameter, this is equivalent to finding a specific value for the perturbation $D_n^{(1)} = -\int_0^1 F(\hat{\ell})d\hat{\ell}$. If we make the simplest choice that the rate premultiplier k is a constant, then the integral, defined by the integrand F in (202) can be done analytically and obtains

$$D_n^{(1)} = -\frac{1}{k}\frac{2\gamma^2}{(\gamma+1)^2}\left[\frac{1}{2(1-\nu)} + \frac{2}{3-2\nu} + \frac{1}{2(2-\nu)}\right]. \tag{213}$$

This last formula, combined with (194), is the $D_n - \kappa$ relation for the model explosive.

We now give a final set of (dimensional) formulas that summarize the basic result. For an explosive material modeled by a polytropic equation of state,

$$e = \frac{1}{\gamma - 1}\frac{p}{\rho} - Q\lambda, \tag{214}$$

and a rate late of the form

$$r = k\,(1-\lambda)^\nu \text{ for } 0 \le \nu < 1, \tag{215}$$

the (dimensional) $D_n - \kappa$ relation is given to $O(\kappa)$ by the formula

$$D_n = D_{CJ} - \frac{D_{CJ}^2}{k}\frac{2\gamma^2}{(\gamma+1)^2}\left[\frac{1}{2(1-\nu)} + \frac{2}{3-2\nu} + \frac{1}{2(2-\nu)}\right]\kappa. \tag{216}$$

This representative result for the $D_n - \kappa$ relation and the description of the reaction zone structure, that accompanies it, has become the basis for the engineering Method of Detonation Shock Dynamics, that will be described in a sequel to these lectures.

9 Acknowledgments

These lectures have been written as part of a contract with the U. S. Air Force, Wright Laboratory, Armament Directorate, Eglin Air Force Base, F08630-91-K0057. The lectures were given at Eglin AFB in July 1992. David Wagnon and Joseph Foster were our kind hosts and the organizers of the lecture series. Special thanks to Jin Yao and David Ford for help in proofreading these notes.

References

[1] "Detonation Shock Dynamics (DSD) 'Calibration for PBX 9502'", Bdzil, J. B., Davis, W. C. and Critchfield, R. R., Proceedings of the Tenth Symposium (International) on Detonation, Boston, Mass, 1993, to appear.

[2] Eyring, H., Powell, R. E. Duffy, G. H. Darling, R. B (1949), "The stability of detonations", Chem Rev. 45: 69-181.

[3] Wood, W. W. and Kirkwood J. G., "Diameter effects in condensed explosives: The relation between velocity and radius of curvature" (1954), J. Chem Phys. 22: 1920- 1924.

[4] Bdzil, J. B., "Steady state two-dimensional detonation", Journal of Fluid Mechanics, Vol. 108, 1981, pp. 185-226.

[5] Stewart, D. S. and Bdzil, J. B., "The shock dynamics of stable multidimensional detonation," Combustion and Flame, 72, 311-323 (1988).

[6] Lambourn, B. D., "Application of Whitham's Shock Dynamics to the propagation of divergent detonations", Proceedings of the Ninth Symposium (International) on Detonation, Portland, OR, (1990), pp. 784-797.

[7] Bukiet, B. and Menikoff, R., "Understanding curved detonation waves", Proceedings of the Tenth Symposium (International) on Detonation, Boston, Mass, 1993, to appear.

[8] Rupert Klein and D. S. Stewart, "The relation between curvature, rate state-dependence and detonation velocity" to appear in the SIAM Journal of Applied Mathematics, Oct 1993.

[9] Bdzil, J. B. and Fickett, W., "DSD technology: A detonation reactive Huygens code", Los Alamos National Laboratory Report, LA-12235-MS, 1992.

[10] Swift, D. C. and Lambourn, B. D., "Developments in the W-B-L detonation model", Proceedings of the Tenth Symposium (International) on Detonation, Boston, Mass, 1993, to appear.

[11] Lee, H. I. and Stewart, D. S., "Calculation of Linear Detonation Instability: One-Dimensional Instability of Plane Detonations," Journal of Fluid Mechanics, Vol. 216, 1990, pp.103-132.

[12] Bourlioux, A. , Majda, A. and Roytburd, V., "Theoretical and numerical structure of unstable one-dimensional detonations", SIAM Journal of Applied Mathematics, Vol. 51, 1991, pp 303-343.

[13] Lee, Jaimin, Persson Per-Anders and Bdzil, John B., "Detonation Shock Dynamics of composite energetic materials", submitted for publication.

[14] Fickett, W. and Davis, W. C. *Detonation*, University of California Press, (1979).

[15] Bdzil, J. B. and Stewart, D. S., "Two-dimensional, time dependent detonation: The interaction of edge rarefactions with finite reaction zones," Journal of Fluid Mechanics, Vol. 171, pp. 1-26 (1986).

[16] Bdzil, J. B. and Stewart, D. S., "Modeling of two-dimensional detonation with detonation shock dynamics," Physics of Fluids, A, Vol. 1, No. 7, p. 1261, (1988).

[17] Bdzil, J. B., Fickett, W. and Stewart, D. S., "Detonation shock dynamics: A new approach to modeling multi-dimensional detonation waves," Proceedings of the 9th (International) Symposium on Detonation, Portland, OR, (1990), pp. 730-742.

[18] Stewart, D. S., and Bdzil, J.B., "A lecture on Detonation Shock Dynamics," Mathematical Modeling in Combustion Science, Lecture Notes in Physics, Vol. 249, pp. 17-30, Springer-Verlag Publishers (1988).

[19] Stewart, D. S. and Bdzil, J. B., "Examples of detonation shock dynamics for detonation wave spread applications", Proceedings of the 9th (International) Symposium on Detonation, Portland, OR, (1990), pp. 773-783.

List of Recent TAM Reports

No.	Authors	Title	Date
496	Klein, R., and D. S. Stewart	The relation between curvature, rate state dependence, and detonation velocity	Apr. 1991
497	Powers, J. M., and D. S. Stewart	Approximate solutions for oblique detonations in the hypersonic limit	Apr. 1991
498	Davidson, M. T., K. L. Kuster, K. W. Quinn, N. A. Sluz, and G. Stojkovich	Twenty-fifth student symposium on engineering mechanics, M. E. Clark, coord. (1988)	Feb. 1992
499	Cardenas, H. E., W. C. Crone, D. J. Scott, G. G. Stewart, and B. F. Tatting	Twenty-sixth student symposium on engineering mechanics, M. E. Clark, coord. (1989)	Mar. 1992
700	Juister, C. E., D. W. Newport, C. S. Payne, J. M. Peters, M. P. Thomas, and J. C. Trovillion	Twenty-seventh student symposium on engineering mechanics, M. E. Clark, coord. (1990)	Apr. 1992
701	Bernard, R. T., D. W. Claxon, J. A. Jones, V. R. Nitzsche, and M. T. Stadtherr	Twenty-eighth student symposium on engineering mechanics, M. E. Clark, coord. (1991)	Apr. 1992
702	Greening, L. E., P. J. Joyce, S. G. Martensen, M. D. Morley, J. M. Ockers, M. D. Taylor, and P. J. Walsh	Twenty-ninth student symposium on engineering mechanics, J. W. Phillips, coord. (1992)	May 1992
703	Kuah, H. T., and D. N. Riahi	Instabilities and transition to chaos in plane wakes	Nov. 1992
704	Stewart, D. S., K. Prasad, and B. W. Asay	Simplified modeling of transition to detonation in porous energetic materials	Nov. 1992
705	Stewart, D. S., and J. B. Bdzil	Asymptotics and multi-scale simulation in a numerical combustion laboratory	Jan. 1993
706	Hsia, K. J., Y.-B. Xin, and L. Lin	Numerical simulation of semi-crystalline Nylon 6: Elastic constants of crystalline and amorphous parts	Jan. 1993
707	Hsia, K. J., and J. Q. Huang	Curvature effects on compressive failure strength of long fiber composite laminates	Jan. 1993
708	Jog, C. S., R. B. Haber, and M. P. Bendsoe	Topology design with optimized, self-adaptive materials	Mar. 1993
709	Barkey, M. E., D. F. Socie, and K. J. Hsia	A yield surface approach to the estimation of notch strains for proportional and nonproportional cyclic loading	Apr. 1993
710	Feldsien, T. M., A. D. Friend, G. S. Gehner, T. D. McCoy, K. V. Remmert, D. L. Riedl, P. L. Scheiberle, and J. W. Wu	Thirtieth student symposium on engineering mechanics, J. W. Phillips, coord. (1993)	Apr. 1993
711	Weaver, R. L.	Anderson localization in the time domain: Numerical studies of waves in two-dimensional disordered media	Apr. 1993
712	Cherukuri, H. P., and T. G. Shawki	An energy-based localization theory: Part I—Basic framework	Apr. 1993
713	Manring, N. D., and R. E. Johnson	Modeling a variable-displacement pump	June 1993
714	Birnbaum, H. K., and P. Sofronis	Hydrogen-enhanced localized plasticity—A mechanism for hydrogen-related fracture	July 1993
715	Balachandar, S., and M. R. Malik	Inviscid instability of streamwise corner flow	July 1993
716	Sofronis, P.	Linearized hydrogen elasticity	July 1993
717	Nitzsche, V. R., and K. J. Hsia	Modelling of dislocation mobility controlled brittle-to-ductile transition	July 1993
718	Hsia, K. J., and A. S. Argon	Experimental study of the mechanisms of brittle-to-ductile transition of cleavage fracture in silicon single crystals	July 1993
719	Cherukuri, H. P., and T. G. Shawki	An energy-based localization theory: Part II—Effects of the diffusion, inertia and dissipation numbers	Aug. 1993
720	Aref, H., and S. W. Jones	Chaotic motion of a solid through ideal fluid	Aug. 1993
721	Stewart, D. S.	Lectures on detonation physics: Introduction to the theory of detonation shock dynamics	Aug. 1993